A SHORT FE IMPLEMENTATION FOR A 2D HOMOGENEOUS DIRICHLET PROBLEM OF A FRACTIONAL LAPLACIAN

GABRIEL ACOSTA, FRANCISCO M. BERSETCHE AND JUAN PABLO BORTHAGARAY

ABSTRACT. In [2], a complete n-dimensional finite element analysis of the homogeneous Dirichlet problem associated to a fractional Laplacian was presented. Here we provide a comprehensive and simple 2D $MATLAB^{®}$ finite element code for such a problem. The code is accompanied with a basic discussion of the theory relevant in the context. The main program is written in about 80 lines and can be easily modified to deal with other kernels as well as with time dependent problems. The present work fills a gap by providing an input for a large number of mathematicians and scientists interested in numerical approximations of solutions of a large variety of problems involving nonlocal phenomena in two-dimensional space.

1. INTRODUCTION

The Finite Element Method (FEM) is one of the preferred numerical tools in scientific and engineering communities. It counts with a solid and long established theoretical foundation, mainly in the linear case of second order *elliptic* partial differential equations. These kind of operators, with the Laplacian as a canonical example, are involved in modeling *local* diffusive processes. On the other hand, nonlocal or *anomalous* diffusion models have increasingly impacted upon a number of important areas in science. Indeed, non-local formulations can be found in physical and social contexts, modeling as diverse phenomena as human locomotion in relation to crime diffusion [7], electrodiffusion of ions within nerve cells [12] or machine learning [14].

The Fractional Laplacian (FL) is among the most prominent examples of a non-local operator. For $0 < s < 1$, it is defined as

$$(1.1) \qquad (-\Delta)^s u(x) = C(n,s) \text{ p.v.} \int_{\mathbb{R}^n} \frac{u(x) - u(y)}{|x - y|^{n+2s}} \, dy,$$

1

where

$$C(n, s) = \frac{2^{2s} s \Gamma(s + \frac{n}{2})}{\pi^{n/2} \Gamma(1 - s)}$$

is a normalization constant. The FL, given by (1.1), is one of the simplest pseudo-differential operators and can also be regarded as the infinitesimal generator of a $2s$-stable Lévy process [5].

Given a function f defined in a bounded domain Ω, the homogeneous Dirichlet problem associated to the FL reads: find u such that

$$(1.2) \qquad \begin{cases} (-\Delta)^s u = f & \text{in } \Omega, \\ \qquad\quad u = 0 & \text{in } \Omega^c. \end{cases}$$

In contrast to elliptic PDEs, numerical developments for problems involving this non-local operator, even in simplified contexts, are seldom found in the literature. The reason for that is related to two major challenging tasks usually involved in its numerical treatment: the handling of highly singular kernels and the need to cope with an unbounded region of integration. This is precisely the case of (1.2), for which just a few numerical methods have been proposed. Effectively implemented *in one space dimension*, we mention, for instance: a finite difference scheme by Huang and Oberman [11], a FE approach developed by D'Elia and Gunzburger [8] that relies on a volume-constrained version of the non-local operator and a simple one-dimensional spectral approach [3]. We refer the reader to [2] for a more detailed account of these schemes and a discussion on other fractional diffusion operators on bounded domains and their discretizations.

To the best of the authors' knowledge, numerical computations for (1.2) in higher dimensions have become available only recently [2]. In that paper a complete n-dimensional finite element analysis for the FL has been carried out, including regularity of solutions of (1.2) in standard and weighted fractional spaces. Moreover, the convergence for piecewise linear elements is proved with optimal order for both uniform and graded meshes.

In that work there are presented error bounds in the energy norm and numerical experiments (in 2D), demonstrating an accuracy of the order of $h^{1/2} \log h$ and $h \log h$ for solutions obtained by means of uniform and graded meshes, respectively.

The present article can be seen as a complementary work to [2], providing a short and simple $MATLAB^{\circledR}$ FE code coping with the homogeneous Dirichlet problem (1.2).

In [4] a $MATLAB^{\circledR}$ implementation for *linear* finite elements and *local* elliptic operators is presented in a concise way. We tried to emulate as much as possible that spirit in the non-local context. Notwithstanding that and in spite of our efforts, some intrinsic technicalities make our code inevitably slightly longer and more complex than that. Just to give a hint about it, we take a glimpse in advance at the nonlocal stiffness matrix K. It involves

expressions of the type

$$(1.3) \qquad \int_{\mathbb{R}^2} \int_{\mathbb{R}^2} \frac{(\varphi_i(x) - \varphi_i(y))(\varphi_j(x) - \varphi_j(y))}{|x - y|^{2+2s}} \, dx dy,$$

where φ_i, φ_j are arbitrary nodal basis functions associated to a triangulation $\mathcal{T}$. Two difficulties become apparent in the calculation of (1.3). First, at the element level, computing (1.3) leads to terms like

$$(1.4) \qquad \int_T \int_{\tilde{T}} \frac{(\varphi_i(x) - \varphi_i(y))(\varphi_j(x) - \varphi_j(y))}{|x - y|^{2+2s}} \, dx dy,$$

for arbitrary pairs $T, \tilde{T} \in \mathcal{T}$. If T and $\tilde{T}$ are not neighboring then the integrand in (1.4) is a regular function and can be integrated numerically in a standard fashion. On the other hand, if $T \cap \tilde{T} \neq \emptyset$ an accurate algorithm to compute (1.4) is not easy to devise. Fortunately, (1.4) bears some resemblances to typical integrals appearing in the Boundary Element Method [15] and we extensively exploit this fact. Indeed, a basic and well known technique in the BEM community is to rely on Duffy-type transforms. This approach leads us to the decomposition of such integrals into two parts: a highly singular but explicitly integrable part and a smooth, numerically treatable part. We use this method to show how (1.4) can be handled with an arbitrary degree of precision (this is carefully treated in Appendices A.1, A.2, A.3, A.4).

Yet another difficulty is hidden in the calculation of K. Although Ω is a bounded domain and the number of potential unknowns is always finite, (1.3) involves a computation in $\mathbb{R}^2 \times \mathbb{R}^2$. In particular, in the homogeneous setting, we need to accurately compute the function

$$(1.5) \qquad \int_{\Omega^c} \frac{1}{|x - y|^{2+2s}} \, dy,$$

for any $x \in \Omega$. That, of course, can be hard to achieve for a domain with a complex boundary. Nonetheless, introducing an extended secondary mesh, as it is explained in Section 3, it is possible to reduce such problem to a simple case in which $\partial\Omega$ is a circle. We show that in this circumstance a computation of (1.5) can be both fast and accurately delivered (see also Appendix A.5). Remarkably, this simple idea applies in arbitrary space dimensions.

Regarding the code itself, our main concern has been to keep a compromise between readability and efficiency. First versions of our code were plainly readable but too slow to be satisfactory. In the code offered here many computations have been vectorized and a substantial speed up gained, sometimes at the price of losing (hopefully not too much) readability.

Last but not least, the full program is available from the authors upon request, so that the reader can avoid retyping it. Small modifications of the base code may make it usable for dealing with many different problems.

It has been successfully used in several contexts such as eigenvalue compu-
tations and time dependent problems (considering semi and full fractional
settings), among others.

The paper is organized as follows. In Section 2, we review appropriate
fractional spaces and regularity results for (1.2). Section 3 deals with basic
aspects of the FE setting. The data structure is carefully discussed in Section
4 and the main loop of the code is described in Section 5. Section 6, in
turn, shows a numerical example for which a nontrivial (i.e. with a non
constant source term f) solution is explicitly known. Moreover, the e.o.c. in
$L^2(\Omega)$ is presented for some values of s. These numerical results are in very
good agreement with those expected by using standard duality arguments
together with the theory given in [2]. Appendix A may be found rather
technical for people not coming from the Boundary Element community
and deals with the quadrature rules used in each singular case. Appendices
B and C describe respectively auxiliary functions and data used along the
program. Finally, the full code, including the line numbers, is exhibited in
Appendix D.

2. Function spaces and regularity of solutions

Given an open set $\Omega \subset \mathbb{R}^n$ and $s \in (0,1)$, define the fractional Sobolev
space $H^s(\Omega)$ as

$$H^s(\Omega) = \left\{ v \in L^2(\Omega) \colon |v|_{H^s(\Omega)} < \infty \right\},$$

where $|\cdot|_{H^s(\Omega)}$ is the Aronszajn-Slobodeckij seminorm

$$|v|_{H^s(\Omega)}^2 = \iint_{\Omega^2} \frac{|v(x) - v(y)|^2}{|x - y|^{n+2s}} \, dx \, dy.$$

It is evident that $H^s(\Omega)$ is a Hilbert space endowed with the norm $\|\cdot\|_{H^s(\Omega)} = \|\cdot\|_{L^2(\Omega)} + |\cdot|_{H^s(\Omega)}$. Moreover, consider the bilinear form $\langle \cdot, \cdot \rangle$ on $H^s(\Omega)$,

$$(2.1) \qquad \langle u, v \rangle_{H^s(\Omega)} = \iint_{\Omega^2} \frac{(u(x) - u(y))(v(x) - v(y))}{|x - y|^{n+2s}} \, dx \, dy.$$

Let us also define the space of functions supported in Ω,

$$\widetilde{H}^s(\Omega) = \left\{ v \in H^s(\mathbb{R}^n) \colon \ \mathrm{supp}\, v \subset \bar{\Omega} \right\}.$$

This space may be defined through interpolation,

$$\widetilde{H}^s(\Omega) = \left[L^2(\Omega), H_0^1(\Omega) \right]_s.$$

Moreover, depending on the value of s, different characterizations of this
space are available. If $s < \frac{1}{2}$ then $\widetilde{H}^s(\Omega)$ coincides with $H^s(\Omega)$, and if $s > \frac{1}{2}$
it may be characterized as the closure of $C_0^\infty(\Omega)$ with respect to the $|\cdot|_{H^s(\Omega)}$
norm. In the latter case, it is also customary to denote it by $H_0^s(\Omega)$. The

particular case of $s = \frac{1}{2}$ gives raise to the Lions-Magenes space $H_{00}^{\frac{1}{2}}(\Omega)$, which can be characterized by

$$H_{00}^{\frac{1}{2}}(\Omega) = \left\{ v \in H^{\frac{1}{2}}(\Omega) \colon \int_{\Omega} \frac{v(x)^2}{\mathrm{dist}(x, \partial\Omega)} \, dx < \infty \right\}.$$

Note that the inclusion $H_{00}^{\frac{1}{2}}(\Omega) \subset H_0^{\frac{1}{2}}(\Omega) = H^{\frac{1}{2}}(\Omega)$ is strict. We also need to introduce the dual space of $\widetilde{H}^s(\Omega)$, denoted with the standard negative exponent $H^{-s}(\Omega)$.

It is apparent that the form $\langle \cdot, \cdot \rangle_{H^s(\mathbb{R}^n)}$ (recall (2.1)) induces a norm on $\widetilde{H}^s(\Omega)$, because of the following well known result.

Proposition 2.1 (Poincaré inequality). *There is a constant $c = c(\Omega, n, s)$ such that*

$$\|v\|_{L^2(\Omega)} \leq c|v|_{H^s(\mathbb{R}^n)} \quad \forall v \in \widetilde{H}^s(\Omega).$$

Finally, Sobolev spaces of order grater than 1 are defined in the following way: given $k \in \mathbb{N}$, then

$$H^{k+s}(\Omega) = \left\{ v \in H^k(\Omega) \colon |D^\alpha v| \in H^s(\Omega) \, \forall \alpha \text{ with } |\alpha| = k \right\},$$

furnished with the norm

$$\|v\|_{H^{k+s}(\Omega)} = \|v\|_{H^k(\Omega)} + \sum_{|\alpha|=k} |D^\alpha v|_{H^s(\Omega)}.$$

Weak solutions of (1.2) are straightforwardly defined multiplying by a test function and integrating by parts. Indeed, the weak formulation of (1.2) reads: find $u \in \widetilde{H}^s(\Omega)$ such that

$$(2.2) \qquad \frac{C(n,s)}{2} \langle u, v \rangle_{H^s(\mathbb{R}^n)} = \int_{\Omega} fv, \quad v \in \widetilde{H}^s(\Omega).$$

Notice that the inner product

$$(2.3) \qquad \langle u, v \rangle_{H^s(\mathbb{R}^n)} = \iint_{\mathbb{R}^n \times \mathbb{R}^n} \frac{(u(x) - u(y))(v(x) - v(y))}{|x - y|^{n+2s}} \, dx \, dy.$$

involves integrals in $\mathbb{R}^n$.

From now on, we assume $f \in H^r(\Omega)$ for some $r \geq -s$. Existence and uniqueness of solutions in $\widetilde{H}^s(\Omega)$ and well-posedness of problem (2.2) are immediate consequences of the Lax-Milgram lemma. Moreover, the following regularity result is valid [10, 16]:

Theorem 2.2. *Let $u \in \widetilde{H}^s(\Omega)$ be the solution to (2.2). If $\partial\Omega$ is of C^∞ class, then*

$$u \in \begin{cases} H^{2s+r}(\Omega) & \text{if } s + r < 1/2, \\ H^{s+1/2-\varepsilon}(\Omega) \, \forall \varepsilon > 0 & \text{if } s + r \geq 1/2. \end{cases}$$

Remark 2.3. The previous theorem implies that, independently of the regularity of the right hand side function f, solutions should not be expected to have derivatives of order greater than $s + 1/2$ in $L^2(\Omega)$. This is a consequence of the behavior of solutions near the boundary of Ω: the quotient $u(x)/d(x, \partial\Omega)^s$ can be shown to be finite for $x \sim \partial\Omega$ (see, for example [13]). Knowledge of this singularity was exploited in [2], where problem (2.2) was set up in the framework of weighted Sobolev spaces and solutions were proved to have $1 + s - \varepsilon$ derivatives in a suitable space if the right hand side function belongs to $C^{1-s}(\Omega)$. See that work for further details.

3. FE SETTING

Consider an admissible triangulation $\mathcal{T}$ of Ω consisting of $N_{\mathcal{T}}$ elements. For the discrete space $\mathbb{V}_h$, we take standard *continuous* piecewise linear elements over $\mathcal{T}$. With the usual notation, we introduce the nodal basis $\{\varphi_1, \ldots, \varphi_N\} \subset \mathbb{V}_h$ corresponding to the internal nodes $\{x_1, \ldots, x_N\}$, that is $\varphi_i(x_j) = \delta_i^j$. Given an element $T \in \mathcal{T}$, we denote by h_T and ρ_T its diameter and inner radius, respectively. As customary, we write $h = \max_{T \in \mathcal{T}} h_T$. The family of triangulations considered is assumed to be shape-regular, namely, there exists $\sigma > 0$ independent of $\mathcal{T}$ such that

$$h_T \leq \sigma \rho_T \text{ for all } T \in \mathcal{T}.$$

In this context, the discrete analogous of (2.3) reads: find $u_h \in \mathbb{V}_h$ such that

$$(3.1) \qquad \frac{C(n,s)}{2} \langle u_h, v_h \rangle_{H^s(\mathbb{R}^n)} = \int_\Omega f v_h, \quad v_h \in \mathbb{V}_h,$$

providing a *conforming*[1] FEM for any $0 < s < 1$.

Writing the discrete solution as $u_h = \sum_j u_j \varphi_j$, problem (3.1) is equivalent to solving the linear system

$$(3.2) \qquad\qquad\qquad KU = F,$$

where the coefficient matrix $K = (K_{ij}) \in \mathbb{R}^{N \times N}$ and the right-hand side $F = (f_j) \in \mathbb{R}^N$ are defined by

$$K_{ij} = \frac{C(n,s)}{2} \langle \varphi_i, \varphi_j \rangle_{H^s(\mathbb{R}^n)}, \quad f_j = \int_\Omega f \varphi_j,$$

and the unknown is $U = (u_j) \in \mathbb{R}^N$.

The *fractional* stiffness matrix K is symmetric and positive definite, so that (3.2) has a unique solution. Notice that the integrals in the inner product involved in computation of K_{ij} should be carried over $\mathbb{R}^n$. For this reason we find it useful to consider a ball B containing Ω and such that the distance from $\bar{\Omega}$ to B^c is an arbitrary positive number. As it is explained in Appendix A.5, this is needed in order to avoid difficulties caused by lack

---

[1]Notice that even P_0 elements are conforming for $0 < s < 1/2$. We restrict ourselves to continuous P_1 in order to give an unified conforming approach for any $0 < s < 1$.

of symmetry when dealing with the integral over Ω^c when Ω is not a ball. Together with B, we introduce an auxiliary triangulation $\mathcal{T}_A$ on $B \setminus \Omega$ such that the complete triangulation $\tilde{\mathcal{T}}$ over B (that is $\tilde{\mathcal{T}} = \mathcal{T} \cup \mathcal{T}_A$) is admissible (see Figure 1).
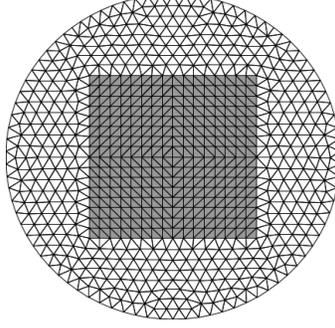
FIGURE 1. A square domain Ω (gray) and an auxiliary ball containing it. Regular triangulations $\mathcal{T}$ and $\mathcal{T}_A$ for Ω and $B \setminus \Omega$ are shown. The final symmetry of the admissible triangulation $\tilde{\mathcal{T}} = \mathcal{T} \cup \mathcal{T}_A$, exhibited in the example, is not relevant.

Let us call $N_{\tilde{\mathcal{T}}}$ the number of elements on the triangulation of B. Then, defining for $1 \le \ell, m \le N_{\tilde{\mathcal{T}}}$ and $1 \le \ell \le N_{\tilde{\mathcal{T}}}$

$$I_{\ell,m}^{i,j} = \int_{T_\ell} \int_{T_m} \frac{(\varphi_i(x) - \varphi_i(y))(\varphi_j(x) - \varphi_j(y))}{|x-y|^{2+2s}} \, dxdy,$$

(3.3)

$$J_\ell^{i,j} = \int_{T_\ell} \int_{B^c} \frac{\varphi_i(x)\varphi_j(x)}{|x-y|^{2+2s}} \, dydx,$$

we may write

$$K_{ij} = \frac{C(n,s)}{2} \sum_{\ell=1}^{N_{\tilde{\mathcal{T}}}} \left(\sum_{m=1}^{N_{\tilde{\mathcal{T}}}} I_{\ell,m}^{i,j} + 2J_\ell^{i,j} \right).$$

As mentioned above, the computation of each integral $I_{\ell,m}^{i,j}$ and $J_\ell^{i,j}$ is challenging for different reasons: the former involves a singular integrand if $\overline{T_\ell} \cap \overline{T_m} \ne \emptyset$ (Appendices A.2, A.3, A.4 are devoted to handle it) while the latter needs to be calculated on an unbounded domain. In this case notice that

$$J_\ell^{i,j} = \int_{T_\ell} \varphi_i(x)\varphi_j(x)\psi(x) \, dx,$$

with $\psi(x) := \int_{B^c} \frac{1}{|x-y|^{2+2s}} \, dy$. Therefore all we need is an accurate computation of $h(x)$ for each quadrature point used in $T_\ell \subset \bar{\Omega}$ (notice that $h(x)$ is a smooth function up to the boundary of Ω since $|x - y| > dist(\bar{\Omega}, B^c) > 0$).

Taking this into account, we observe that it is possible to take advantage of the fact that $h(x)$ is a radial function that can be either quickly computed

on the fly or even precomputed with an arbitrary degree of precision (see Appendix A.5 for a full treatment of $h(x)$).

For the reader's convenience we finish this section with Table 1, containing some handy notations.

TABLE 1. Main Variables

Notation	Meaning
$\mathcal{T}, \mathcal{T}_A, \tilde{\mathcal{T}}$	Meshes: of Ω, $B \setminus \Omega$ and B resp.
$\mathcal{N}$	Nodes of $\mathcal{T}$
$\mathcal{E}$	Edges of $\mathcal{T}$
$\mathcal{B}$	Boundary edges of $\mathcal{T}$
$N_{\mathcal{T}}$	$\#\mathcal{T}$
$N_{\mathcal{N}}$	$\#\mathcal{N}$
$N_{\mathcal{B}}$	$\#\mathcal{B}$

4. DATA STRUCTURE AND AUXILIARY VARIABLES

We assume that the mesh $\mathcal{T}$ has been generated in advance[2]. The information related to $\mathcal{T}$ should be encoded in some specific variables `p`, `t`, `bdrynodes`, `nt_aux nf R`, as follows:

- `p` is a $2 \times N_{\mathcal{N}}$ array, such that `p(:,n)` are the coordinates of the `n`-th node.
- `t` is a $N_{\tilde{\mathcal{T}}} \times 3$ index array, and `t(l,:)` are the indices of the vertices of T_l. Triangles belonging to $\mathcal{T}_A$ must be listed at the end.
- `nt_aux` $= \#\mathcal{T}_A$.
- `bdrynodes` is an index column vector listing the nodes lying on $\partial\Omega$.
- `nf` is an index column vector contiaining the free nodes (those in Ω).
- `R` the radius of B.

These data have to be available in the $MATLAB^{\circledR}$ workspace before the execution of the main code.

Next, we begin by creating some variables that refer to problem (1.2):

```
s = 0.5;
f = @(x,y) 1;
cns = s*2^(-1+2*s)*gamma(1+s)/(pi*gamma(1-s));
load('data.mat');
```

Here, `s` is the order of the fractional Laplacian involved, `f` is a function handle containing the volume force (which as an example we have set to be $f \equiv 1$), and `cns` is equal to the constant $C(n, s)$ previously defined.

---

[2]For the sake of convenience an stored example mesh -as well as a suitable mesh generator- is provided together with the source code.

In order to compute the stiffness matrix we need to estimate the bilinear form $\langle \cdot, \cdot \rangle_{H^s(\mathbb{R}^n)}$ evaluated at the nodal basis through an appropriate quadrature rule.

To perform an efficient vectorized computation, we require some precalculated data, given in the file `data.mat`. This file contains information about nodes and weights for the quadratures performed throughout the code. The content of `data.mat` is listed in Table 2 and further details can be found in Appendix C.

TABLE 2. Variables stored in `data.mat`

Name	Size	Used as input in function:	Description
`p_cube`	27x3	`vertex_quad` `edge_quad`	Quadrature points over $[0,1]^3$
`p_T_6`	6x2	None (used in non-touching case)	Quadrature points over $\hat{T}$
`p_T_12`	12x2	`comp_quad`	Quadrature points over $\hat{T}$
`p_I`	9x1	`comp_quad` `triangle_quad`	Quadrature points over $[0,1]$
`w_I`	9x1	`comp_quad`	Quadrature weights associated to `p_I`
`phiA` `phiB` `phiD`	9x36	None (used in non-touching case)	See Appendix C.2
`vpsi1` `vpsi2`	25x27	`vertex_quad`	See Appendix C.3
`epsi1` `epsi2` `epsi3` `epsi4` `epsi5`	16x27	`edge_quad`	See Appendix C.4
`tpsi1` `tpsi2` `tpsi3`	9x9	`triangle_quad`	See Appendix C.5
`cphi`	9x12	`comp_quad`	See Appendix C.6

As mentioned before, some auxiliary elements are added to the original mesh in order to have a triangulation on a ball B containing Ω (see Figure 1). The nodes in this auxiliary domain $B \backslash \Omega$ are regarded as Dirichlet nodes.

Next, we define some mesh parameters and set to zero the factors involved in equation (3.2). The following lines do not need extra explanation beyond the in-line comments:

```
nn = size(p,2); % number of nodes
nt = size(t,1) % number of elements
uh = zeros(nn,1); % discrete solution
K  = zeros(nn,nn); % stiffness matrix
b  = zeros(nn,1); % right hand side
```

Then, the measures of all the elements in the mesh are calculated:

```
area = zeros(nt,1);
for i=1:nt
    aux = p( : , t(i,:) );
    area(i) = 0.5.*abs(...
        det([ aux(:,1) - aux(:,3)  aux(:,2) - aux(:,3)]) );
end
```

So, `area` is a vector of length $N_{\widetilde{\mathcal{T}}}$ satisfying `area(l)` $= |T_{\mathtt{l}}|$, $\mathtt{l} \in \{1, ..., N_{\widetilde{\mathcal{T}}}\}$.

The quadratures we employ to compute the integrals $I_{\ell,m}^{i,j}$ (defined in (3.3)) depend on whether the elements T_ℓ and T_m coincide or their intersection is an edge, a vertex or empty. Therefore, it is important to distinguish theses cases in an efficient way. We construct a data structure called `patches` as follows, using a linear number of operations:

```
deg = zeros(nn,1);
for i=1:nt
    deg( t(i,:) ) = deg( t(i,:) ) + 1;
end
patches = cell(nn , 1);
for i=1:nn
    patches{i} = zeros( 1 , deg(i) );
end
for i=1:nt
    patches{ t(i,1) }(end - deg( t(i,1) ) + 1) = i;
    patches{ t(i,2) }(end - deg( t(i,2) ) + 1) = i;
    patches{ t(i,3) }(end - deg( t(i,3) ) + 1) = i;
    deg( t(i,:) ) = deg( t(i,:) ) - 1;
end
```

The output of this code block is a $N_{\widetilde{\mathcal{N}}} \times 1$ cell, called `patches`, such that `patches{n}` is a vector containing the indices of all the elements in the neighborhood of the node `n`.

5. Main loop

One of the main challenges to build up a FE implementation to problem (1.2) is to assemble the stiffness matrix in an efficient mode. Independently of whether the supports of two given basis functions φ_i and φ_j are disjoint, the interaction $\langle \varphi_i, \varphi_j \rangle_{H^s(\mathbb{R}^n)}$ is not null. This yields a paramount difference between FE implementations for the classical and the fractional Laplace operators; in the former the stiffness matrix is sparse, while in the latter it is

full. Therefore, unless some care is taken, the amount of memory required and the number of operations needed to assembly the stiffness matrix increases quadratically with the number of nodes. Due to this, the code we present takes advantage of vectorized operations as much as possible.

Moreover, as the computation of the entries of the stiffness matrix requires calculating integrals on *pairs* of elements, it is required to perform a double loop. It is simple to check the identity $I_{\ell,m}^{i,j} = I_{m,\ell}^{i,j}$ for all i, j, ℓ, m, and therefore it is enough to carry the computations only for the pairs of elements T_ℓ and T_m with $\ell \leq m$.

In the following lines we preallocate memory and create the auxiliary index array `aux_ind` (to be used in code line 58).

```
vl = zeros(6,2);
vm = zeros(6*nt,2);
norms = zeros(36,nt);
ML = zeros(6,6,nt);
empty = zeros(nt,1);
aux_ind = reshape( repmat( 1:3:3*nt , 6 , 1 ) , [] , 1 );
empty_vtx = zeros(2,3*nt);
BBm = zeros(2,2*nt);
```

The main loop goes through all the elements T_ℓ of the mesh of Ω, namely, $1 \leq \ell \leq N_{\mathcal{T}}$. Observe that auxiliary elements are excluded from it. Fixed ℓ, the first task is to classify all the mesh elements T_m ($1 \leq m \leq N_{\tilde{\mathcal{T}}}$, $m \neq \ell$) according to whether $\overline{T_\ell} \cap \overline{T_m}$ is empty, a vertex or an edge. This is accomplished employing a linear number of operations by using the `patches` data structure as follows:

```
edge =  [ patches{t(l,1)} patches{t(l,2)} patches{t(l,3)} ];
[nonempty M N] = unique( edge , 'first' );
edge(M) = [];
vertex = setdiff(  nonempty , edge  );
ll = nt - l + 1 - sum( nonempty>=l );
edge( edge<=l ) = [];
vertex( vertex<=l ) = [];
empty( 1:ll ) = setdiff_( l:nt , nonempty );
empty_vtx(:  , 1:3*ll) = p( :  , t( empty(1:ll) , : )' );
```

At this point, `ll` is the number of elements –including the auxiliary ones– whose intersection with T_ℓ is empty and have not been visited yet (namely, those with index `m>l`). By considering only the elements with index greater than ℓ, we are taking advantage of the symmetry of the stiffness matrix. The arrays `empty`, `vertex` and `edge` contain the indices of all those elements whose intersection with T_ℓ is empty, a vertex or an edge respectively, and have not been computed yet. In `empty_vtx` we store the coordinates of the vertices of the triangles indexed in `empty`.

Then, the code proceeds to assemble the right hand side vector in equation (3.2)

```
nodl = t(l,:);
xl = p(1 , nodl); yl = p(2 , nodl);
Bl = [xl(2)-xl(1) yl(2)-yl(1); xl(3)-xl(2) yl(3)-yl(2)]';
b(nodl) = b(nodl) + fquad(area(l),xl,yl,f);
```

Here, `nodl` stores the indices of the vertices of T_ℓ; `xl` and `yl` are the x and y coordinates of these vertices, respectively. The element T_ℓ is the image of a reference element $\hat{T}$ via an affine transformation,

$$(\hat{x}, \hat{y}) \mapsto \texttt{Bl}(\hat{x}, \hat{y}) + (\texttt{xl(1)}, \texttt{yl(1)}).$$

Recall that `b` stores the numerical approximation to the right hand side vector from equation (3.2), namely, $\texttt{b(j)} \approx \int_\Omega f\varphi_j$. The routine `fquad` uses a standard quadrature rule, interpolating f on the edge midpoints of T_l (see Appendix B).

Remark 5.1. Let $1 \leq \ell, m \leq \mathcal{N}_{\tilde{T}}$. When computing $I_{\ell,m}^{i,j}$ or $J_\ell^{i,j}$, the basis function indices i and j do not refer to a global numbering but to a local one. This means, for example, that if $\overline{T_\ell} \cap \overline{T_m} = \emptyset$, then $1 \leq i, j \leq 6$. See Remark A.1 for details on this convention.

5.1. **Identical elements.** The first interaction to be computed by the code corresponds to the case $m = \ell$ in (3.3). The values calculated are assembled in the stiffness matrix K.

```
K(nodl, nodl) = K(nodl, nodl) +...
triangle_quad(Bl,s,tpsi1,tpsi2,tpsi3,area(l),p_I) +...
comp_quad(Bl,xl(1),yl(1),s,cphi,alpha*R,area(l),p_I,w_I,p_T_12);
```

The function `triangle_quad` estimates $I_{\ell,\ell}^{i,j}$, while `comp_quad` computes numerically the value of $J_\ell^{i,j}$. These functions use pre-built data from the file `data.mat`: the first one employs the variables `tpsi1`, `tpsi2` and `tpsi3`, and the second one `cphi`, `p_I`, `w_I` and `p_T_12`. Implementation details can be found in appendixes A.4 and A.5, respectively. The output of both `triangle_quad` and `comp_quad` are 3 by 3 matrices, such that:

$$\texttt{triangle\_quad}_{ij} \approx I_{\ell,\ell}^{i,j}, \quad \texttt{comp\_quad}_{ij} \approx 2J_\ell^{i,j}.$$

5.2. **Non-touching elements.** The next step is to compute the interactions between T_ℓ and all the elements T_m whose closure is disjoint $\overline{T_\ell}$ (so that their indices are stored in the variable `empty`). In order to do this, we calculate and store quadrature points for all the triangles involved in the operation as follows:

```
BBm(:,1:2*ll) = reshape( [ empty_vtx( : , 2:3:3*ll ) -...
  empty_vtx( : , 1:3:3*ll ) , ...
  empty_vtx( : , 3:3:3*ll ) -...
  empty_vtx( : , 2:3:3*ll ) ] , [] , 2)' ;
```

```
vl = p_T_6*(Bl') + [ ones(6,1).*xl(1) ones(6,1).*yl(1) ];
vm(1:6*ll,:) = reshape( permute( reshape( p_T_6*BBm(:,1:2*ll), ...
 [6 1 2 ll] ) , [1 4 3 2] ) , [ 6*ll 2 ] ) +...
 empty_vtx(: , aux_ind(1:6*ll) )';
```

The matrix BBm has size $2 \times 2*$nt, and it contains nt submatrices of dimension 2×2. The m-th submatrix corresponds to the affine transformation that maps $\hat{T}$ into T_m. The vectors vl and vm contain the coordinates of all quadrature points in T_ℓ and T_m for $m \in$ empty, respectively.

Here, the matrix BBm satisfies

$$\texttt{BBm(:,2*m-1:2m)'} \cdot \hat{T} + \texttt{empty\_vtx(:,3*(m-1) + 1)'} \mapsto T_m,$$

The matrix p_T_6 $\in \mathbb{R}^{6 \times 2}$ was provided by the precomputed file data.mat, and it stores the coordinates of the 6 quadrature points in the reference element $\hat{T}$. In order to compute vm, we use three nested operations over the $6 \times 2*$ll matrix p_T_6*BBm(:,1:2*ll). To better understand this, suppose we rewrite this matrix as follows:

$$\texttt{p\_T\_6*BBm(:,1:2*ll)} = [A_1, A_2, ..., A_{\texttt{ll}}],$$

where A_i is a 6×2 matrix and $i = 1, .., $ll. Then, after the application of reshape(permute(reshape(... ', we obtain the 6*ll by 2 matrix $[A_1; A_2; ...; A_{\texttt{ll}}]$, which can be used as an input in pdist2. This trick was taken out from [1].

Next, we compute distances from all the quadrature nodes in vl to the ones in vm, and raise them to the power of $-(2 + 2s)$:

```
norms(:,1:ll) = reshape(pdist2(vl,vm(1:6*ll,:)),36,[]).^(-2-2*s);
```

Thereby, norms is a $36 \times$ ll matrix such that for $m \in \{1, ..., \texttt{ll}\}$,

$$\texttt{norms(:,m)} = \begin{pmatrix} ||\texttt{vl(1,:)} - \texttt{vm(6*m - 5,:)} ||^{-(2+2s)} \\ \vdots \\ ||\texttt{vl(1,:)} - \texttt{vm(6*m, :)} ||^{-(2+2s)} \\ ||\texttt{vl(2,:)} - \texttt{vm(6*m - 5,:)} ||^{-(2+2s)} \\ \vdots \\ ||\texttt{vl(2,:)} - \texttt{vm(6*m, :)} ||^{-(2+2s)} \\ \vdots \\ ||\texttt{vl(6,:)} - \texttt{vm(6*m - 5,:)} ||^{-(2+2s)} \\ \vdots \\ ||\texttt{vl(6,:)} - \texttt{vm(6*m, :)} ||^{-(2+2s)} \end{pmatrix},$$

where $|| \cdot ||$ denotes the usual euclidean distance in $\mathbb{R}^2$.

At this point, we have collected all the necessary information to compute $I_{\ell,m}^{i,j}$ for $\overline{T_\ell} \cap \overline{T_m} = \emptyset$ and i, j corresponding to any of the six vertices of these elements. We employ the pre-built matrices phiA, phiB and phiD, that

contain the values of the nodal basis functions evaluated at the quadrature points of $\hat{T}$, multiplied by their respective weights, and stored in an appropriate way in order to perform an efficient vectorized operation. Details are provided in appendixes A.1 and C.2. The code proceeds:

```
ML(1:3,1:3,1:ll) =  reshape( phiA*norms(:,1:ll) , 3 , 3 , [] );
ML(1:3,4:6,1:ll) =  reshape( phiB*norms(:,1:ll) , 3 , 3 , [] );
ML(4:6,4:6,1:ll) =  reshape( phiD*norms(:,1:ll) , 3 , 3 , [] );
ML(4:6,1:3,1:ll) =  permute( ML(1:3,4:6,1:ll) , [2 1 3] ) ;
```

So, the matrix ML satisfies

$$I_{\ell,m}^{i,j} \approx 4|T_\ell||T_m| \, \texttt{ML(i,j,m)}.$$

The last step to complete the computations for the case $\overline{T_\ell} \cap \overline{T_m} = \emptyset$ is to add the calculated values in their corresponding stiffness matrix entries:

```
for m=1:ll
    order = [nodl t( empty(m) , : )];
    K(order,order) = K(order,order) +...
    ( 8*area(empty(m))*area(l) ).*ML(1:6,1:6,m);
end
```

The vector `order` collects the local indices of the vertices of T_ℓ and T_m, given as explained in Remark A.1. Recall that $I_{\ell,m}^{i,j} = I_{m,\ell}^{i,j}$ and that we are summing over the elements listed in `empty`. In particular, this means that $\ell < m$. We multiply `ML(1:6,1:6,m)` by `8*area(empty(m))*area(l)` instead of by `4*area(empty(m))*area(l)` in order to avoid carrying the redundant computation of $I_{m,\ell}^{i,j}$.

5.3. **Vertex-touching elements.** In order to compute $I_{\ell,m}^{i,j}$ for the indices m corresponding to elements sharing a vertex with T_ℓ, we use the pre-built variables `vpsi1`, `vpsi2` and `p_cube` as input in the function `vertex_quad`. Let us mention once more that `vpsi1` and `vpsi2` contain the nodal basis in the reference element $\hat{T}$ evaluated at quadrature points, multiplied by their respective weight and properly stored. Moreover, the variable `p_cube` stores quadrature nodes in the unit cube $[0, 1]^3$. Further details about `vertex_quad` and the auxiliary pre-built data can be found in appendixes A.2 and C.3, respectively. We compute the integrals and add the resulting values to K as follows:

```
for m=vertex
    nodm = t(m,:);
    nod_com = intersect(nodl, nodm);
    order = [nod_com nodl(nodl~=nod_com) nodm(nodm~=nod_com)];
    K(order,order) = K(order,order) ...
    + 2.*vertex_quad(nodl,nodm,nod_com,p,s,vpsi1,vpsi2,...
    area(l),area(m),p_cube);
end
```

Here, we store in `nodm` the indices of the vertices of T_m, whereas `nod_com` dentoes the index of the vertex shared by T_ℓ and T_m. The first entry of `order` is the index of this common vertex, followed by the nodes of T_ℓ different from it, and then by the indices of the remaining two nodes of T_m. Observe that, unlike the previous case, here there are involved five nodal basis, so the output of `vertex_quad` is a 5 by 5 array, such that:

$$\texttt{vertex\_quad}_{ij} \approx I_{\ell,m}^{i,j}.$$

5.4. **Edge-touching elements.** Proceeding similarly, we compute next the case where $\overline{T_\ell} \cap \overline{T_m}$ is an edge. Now there are only 4 nodal basis functions involved, and the local numbering is such that the first two nodes correspond to the endpoints of the shared edge, the third is the one in T_ℓ but not in T_m and the last one is the node in T_m but not in T_ℓ. Using the pre-built variables `epsi1`, `epsi2`, `epsi3`, `epsi4`,`epsi5` and `p_cube` as input in `edge_quad` (see appendixes A.3 and C.4), we proceed as in the previous case:

```
for m=edge
    nodm = t(m,:);
    nod_diff = [setdiff(nodl, nodm) setdiff(nodm, nodl)];
    order = [ nodl( nodl~=nod_diff(1) ) nod_diff  ];
    K(order,order) = K(order,order) +...
    2.*edge_quad(nodl,nodm,nod_diff,p,s,...
    epsi1,epsi2,epsi3,epsi4,epsi5,area(l),area(m),p_cube);
end
```

The indices of the two nodes not shared by T_ℓ and T_m are stored in `nod_diff`, and `order` has the nodes ordered as explained in the previous paragraph. The output of the function `edge_quad` is a 4 by 4 array satisfying

$$\texttt{edge\_quad}_{ij} \approx I_{\ell,m}^{i,j}.$$

5.5. **Discrete solution.** Once the main loop is concluded, the stiffness matrix `K` and the right hand side vector `b` have been computed, and thus it is possible to calculate the FE solution `uh` of the system (3.2):

```
uh(nf) = ( K(nf,nf)\b(nf) )./cns; % Solving linear system
```

The entries of `K` and `b` needed are only the ones corresponding to free nodes. The nodes belonging to $\partial\Omega$ and to the auxiliary domain $B \setminus \Omega$ are excluded, as the discrete solution `uh` is set to vanish on them.

Finally, `uh` is displayed, and the auxiliary domain is excluded from the representation:

```
trimesh(t(1:nt-nt_aux , :), p(1,:),p(2,:),uh);
```

6. Numerical Experiments

In order to illustrate the performance of the code, in this section we show the results we obtained in an example problem. Explicit solutions for (1.2)

are scarce, but it is possible to obtain a family of them if Ω is a ball. Other numerical experiments carried with this code can be found in [2] and in [6] (for the eigenvalue problem in several domains).

According to the theory given in [2, 6] convergence in the energy norm is expected to occur with order $\frac{1}{2}$ with respect to the mesh size parameter h, or equivalently, of order $-\frac{1}{2n}$ with respect to the number of degrees of freedom. Moreover, using duality arguments, it is expected to have order of convergence $s + \frac{1}{2}$ (resp. $-\frac{s+1/2}{n}$) for $0 < s \leq 1/2$ and 1 (resp. $-\frac{1}{n}$) for $s > 1/2$ in the $L^2(\Omega)$-norm with respect to h (resp. number of degrees of freedom).

We first construct non-trivial solutions for (1.2) if Ω is a ball. Consider the Jacobi polynomials $P_k^{(\alpha,\beta)} : [-1, 1] \to \mathbb{R}$, given by

$$P_k^{(\alpha,\beta)}(z) = \frac{\Gamma(\alpha + k + 1)}{k!\,\Gamma(\alpha + \beta + k + 1)} \sum_{m=0}^{k} \binom{k}{m} \frac{\Gamma(\alpha + \beta + k + m + 1)}{\Gamma(\alpha + m + 1)} \left(\frac{z - 1}{2}\right)^m,$$

and the weight function $\omega^s : \mathbb{R}^n \to \mathbb{R}$,

$$\omega^s(x) = (1 - \|x\|^2)_+^s.$$

In [9, Theorem 3] it is shown how to construct explicit eigenfunctions for an operator closely related to the FL by using $P_k^{(s,n/2-1)}$. To be more precise, the authors prove the following result.

Theorem 6.1. *Let $B(0, 1) \subset \mathbb{R}^n$ the unitary ball. For $s \in (0, 1)$ and $k \in \mathbb{N}$, define*

$$\lambda_{k,s} = \frac{2^{2s}\,\Gamma(1 + s + k)\Gamma\left(\frac{n}{2} + s + k\right)}{k!\,\Gamma\left(\frac{n}{2} + k\right)}$$

and $p_k^{(s)} : \mathbb{R}^n \to \mathbb{R}$,

$$p_k^{(s)}(x) = P_k^{(s,\,n/2-1)}(2\|x\|^2 - 1)\chi_{B(0,1)}(x).$$

Then the following equation holds

$$(-\Delta)^s\left(\omega^s p_k^{(s)}(x)\right) = \lambda_{k,s}\,p_k^{(s)}(x) \ in \ B(0, 1).$$

A family of explicit solutions is available by using this theorem. As a first example, we analyze the solution with $k = 0$. This gives a right hand side equal to a constant. Namely, consider

(6.1) $\begin{cases} (-\Delta)^s u = 1 & \text{in } B(0, 1) \subset \mathbb{R}^2, \\ \qquad\quad u = 0 & \text{in } B(0, 1)^c. \end{cases}$

We have run the code for a wide range of parameters s, while keeping the radius of the auxiliary ball B equal to 1.1. Orders of convergence in the L^2 and energy norm[3] are shown in Table 3; these results are in accordance with the theory.

---

[3]A discussion about how to compute errors in the energy norm can be found in [2].

TABLE 3. Computational rates of convergence for problem (6.1) with respect to the mesh size, measured in the $L^2(\Omega)$ and energy norms.

Value of s	Order in $L^2(\Omega)$	Order in $\widetilde{H}^s(\Omega)$
0.1	0.621	0.500
0.2	0.721	0.496
0.3	0.804	0.492
0.4	0.880	0.491
0.5	0.947	0.492
0.6	1.003	0.496
0.7	1.046	0.501
0.8	1.059	0.494
0.9	0.999	0.467

As a second example we illustrate, in Table 4, that in problem (6.1) the radius R of the auxiliary ball B does not substantially affect the error of the scheme. This suggests that it is preferable to maintain the exterior ball's radius as small as possible. Since in this problem the domain Ω is itself a ball, for comparison, we also included the output of the code without resorting to the exterior ball (the row corresponding to $R = 1.0$). The table clearly shows that the CPU time grows linearly with respect to the number of elements $N_{\widetilde{\mathcal{T}}} - N_{\mathcal{T}}$ used in the auxiliary domain. Taking into account that the final size of the linear system (3.2) involved in each case is the same, the computational cost is, essentially, increased only during the assembling routine. Since considering an auxiliary domain involves only the computation of the interaction between inner and outer nodes, a linear behavior of the type described above is clearly expected.

TABLE 4. The $L^2(\Omega)$ and $\widetilde{H}^s(\Omega)$ errors for different values of R in problem (6.1) with $s = 0.5$. In all the cases we are using a fixed and regular triangulation $\mathcal{T}$ of Ω, with $N_{\mathcal{T}} = 4228$. The computations were performed with $MATLAB^{\circledR}$ version 2015a in Windows 10, Intel i7 Processor, RAM 8Gb.

R	$N_{\widetilde{\mathcal{T}}}$	CPU time (sec.)	Error in $\|\cdot\|_{L^2(\Omega)}$	Error in $\|\cdot\|_{\widetilde{H}^s(\Omega)}$
1.0	4228	80.3	0.0164	0.1314
1.1	4980	100.7	0.0167	0.1345
1.4	8218	206.6	0.0167	0.1351
1.7	12370	344.7	0.0167	0.1352
2.0	17170	511.9	0.0167	0.1354

As a third example we return to the setting of Theorem 6.1. We consider $k = 2$ and compute the order of convergence in $L^2(\Omega)$ for $s = 0.25$ and $s = 0.75$. We summarize our numerical results in Figure 2. These are in accordance with the predicted rates of convergence. Finally, in Figure 3 the

FE solution, for $s = 0.75$ and $k = 2$, computed with a mesh of about 14000 triangles is displayed.
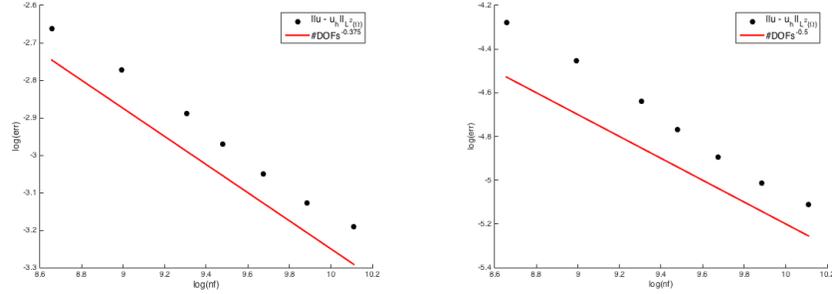
FIGURE 2. Computational rate of convergence in the $L^2(\Omega)$-norm for the problem with solution given by Theorem 6.1, for $k = 2$. The left panel corresponds to $s = 0.25$ and the right to $s = 0.75$. The *asymptotic* rate for $s = 0.25$ is $\approx (\#\mathrm{DOFs})^{-3/8}$, whereas for $s = 0.75$ it is $\approx (\#\mathrm{DOFs})^{-1/2}$, in agreement with theory.
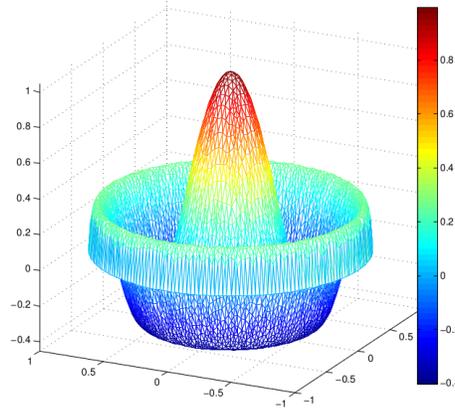
FIGURE 3. FE solution with a mesh containing about 14000 triangles. With $s = 0.75$, we use $f(x) = \lambda_{2,0.75}\, p_2^{(0.75)}(x)$ as a source term (see Theorem 6.1).

Finally, we would like to mention just a few more facts: our numerical experiments suggest that the condition number of K behaves like $\sim N_{\mathcal{T}}^s$ while over the 99% of the CPU time is devoted to the assembly routine. Actually, the expected complexity for assembling K is quadratic in the number of elements, and this seems to be the case in our tests.

APPENDIX A. QUADRATURE RULES

Here we give details about how to compute the integrals $I_{\ell,m}^{i,j}$ and $J_{\ell}^{i,j}$ (see Section 3). In order to cope with $I_{\ell,m}^{i,j}$, we proceed according to whether $\overline{T_\ell} \cap \overline{T_m}$ is empty, a vertex, an edge or an element. Recall that $I_{\ell,m}^{i,j} = I_{m,\ell}^{i,j}$, so that we may assume $\ell \leq m$.

Consider two elements T_ℓ and T_m such that $\mathrm{supp}(\varphi_i), \mathrm{supp}(\varphi_j) \cap (T_\ell \cup T_m) \neq \emptyset$. Observe that if one of this intersections is empty, then $I_{\ell,m}^{i,j} = 0$. Moreover, it could be possible that one of the elements is disjoint with the support of both φ_i and φ_j, provided the other element intersects both supports and $I_{\ell,m}^{i,j} \neq 0$.

We are going to consider the reference element

$$\hat{T} = \{\hat{x} = (\hat{x}_1, \hat{x}_2) \colon 0 \leq \hat{x}_1 \leq 1, \, 0 \leq \hat{x}_2 \leq \hat{x}_1\},$$

whose vertices are

$$\hat{x}^{(1)} = \begin{pmatrix} 0 \\ 0 \end{pmatrix}, \quad \hat{x}^{(2)} = \begin{pmatrix} 1 \\ 0 \end{pmatrix}, \quad \hat{x}^{(3)} = \begin{pmatrix} 1 \\ 1 \end{pmatrix}.$$

The basis functions on $\hat{T}$ are, obviously,

$$\hat{\varphi}_1(\hat{x}) = 1 - \hat{x}_1, \quad \hat{\varphi}_2(\hat{x}) = \hat{x}_1 - \hat{x}_2, \quad \hat{\varphi}_3(\hat{x}) = \hat{x}_2.$$

Remark A.1. Given two elements T_ℓ and T_m, we provide a local numbering in the following way. If T_ℓ and T_m are disjoint, we set the first three nodes to be the nodes of T_ℓ and the following three nodes to be the ones of T_m. Else, we set the first node(s) to be the ones in the intersection, then we insert the remaining node(s) of T_ℓ and finally the one(s) of T_m (see Figure 4). For simplicity of notation, when computing $I_{\ell,m}^{i,j}$ and $J_{\ell}^{i,j}$, we assume that i, j denote the local numbering of the basis functions involved; for example, if T_ℓ and T_m share only a vertex, then $1 \leq i, j \leq 5$.
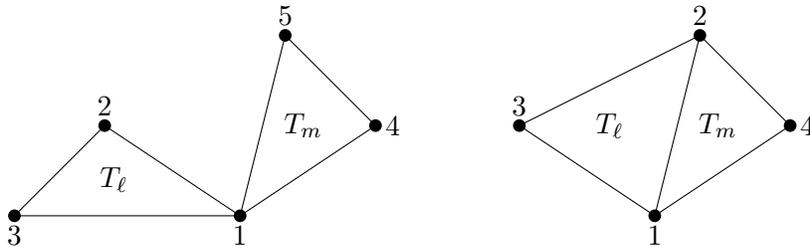
FIGURE 4. Local numbering for elements with a vertex and an edge in common.

Consider the affine mappings

$$\chi_\ell \colon \hat{T} \to T_\ell, \qquad\qquad \chi_\ell(\hat{x}) = B_\ell \hat{x} + x_\ell^{(1)},$$

$$\chi_m : \hat{T} \to T_m, \qquad\qquad \chi_m(\hat{x}) = B_m \hat{x} + x_m^{(1)},$$

where the matrices B_ℓ and B_m are such that $\hat{x}^{(2)}$ (resp. $\hat{x}^{(3)}$) is mapped respectively to the second (resp. third) node of T_ℓ and T_m in the local numbering defined above. Then, it is clear that

(A.1)
$$I_{\ell,m}^{i,j} = 4|T_\ell||T_m| \int_{\hat{T}} \int_{\hat{T}} \frac{(\varphi_i(\chi_\ell(\hat{x})) - \varphi_i(\chi_m(\hat{y})))(\varphi_j(\chi_\ell(\hat{x})) - \varphi_j(\chi_m(\hat{y})))}{|\chi_\ell(\hat{x}) - \chi_m(\hat{y})|^{2+2s}} \, d\hat{x} \, d\hat{y} =$$
$$= 4|T_\ell||T_m| \iiiint_{\hat{T} \times \hat{T}} F_{ij}(\hat{x}_1, \hat{x}_2, \hat{y}_1, \hat{y}_2) \, d\hat{x}_1 \, d\hat{x}_2 \, d\hat{y}_1 \, d\hat{y}_2.$$

We discuss how to compute $I_{\ell,m}^{i,j}$ depending on the relative position of T_ℓ and T_m, and afterwards we tackle the computation of $J_\ell^{i,j}$.

A.1. **Non-touching elements.** This is the simplest case, since the integrand F_{ij} in (A.1) is not singular. Recall that

$$I_{\ell,m}^{i,j} = \int_{T_\ell} \int_{T_m} \frac{(\varphi_i(x) - \varphi_i(y))(\varphi_j(x) - \varphi_j(y))}{|x - y|^{2+2s}} \, dxdy, \quad 1 \le \ell, m \le N_{\tilde{\mathcal{T}}}.$$

Splitting the numerator in the integrand, we obtain

$$I_{\ell,m}^{i,j} = \int_{T_\ell} \int_{T_m} \frac{\varphi_i(x)\varphi_j(x)}{|x - y|^{2+2s}} \, dxdy + \int_{T_\ell} \int_{T_m} \frac{\varphi_i(y)\varphi_j(y)}{|x - y|^{2+2s}} \, dxdy$$
$$- \int_{T_\ell} \int_{T_m} \frac{\varphi_i(x)\varphi_j(y)}{|x - y|^{2+2s}} \, dxdy - \int_{T_\ell} \int_{T_m} \frac{\varphi_i(y)\varphi_j(x)}{|x - y|^{2+2s}} \, dxdy.$$

Note that all the integrands depend on ℓ and m only through their denominators. Since $\varphi_i(x) = 0$ if $i = 1, 2, 3$ and $x \in T_m$ or if $i = 4, 5, 6$ and $x \in T_\ell$, given two indices i, j, only one of the four integrals above is not null. Thus, we may divide the 36 interactions between the 6 basis functions involved into four 3 by 3 blocks, and write the local matrix ML as:

(A.2)
$$\text{ML} = \begin{pmatrix} A_{\ell,m} & B_{\ell,m} \\ C_{\ell,m} & D_{\ell,m} \end{pmatrix},$$

where

$$A_{\ell,m}^{i,j} = \int_{T_\ell} \int_{T_m} \frac{\varphi_i(x)\varphi_j(x)}{|x - y|^{2+2s}} \, dxdy, \qquad B_{\ell,m}^{i,j} = -\int_{T_\ell} \int_{T_m} \frac{\varphi_i(x)\varphi_{j+3}(y)}{|x - y|^{2+2s}} \, dxdy$$
$$C_{\ell,m}^{i,j} = -\int_{T_\ell} \int_{T_m} \frac{\varphi_{i+3}(y)\varphi_j(x)}{|x - y|^{2+2s}} \, dxdy, \quad D_{\ell,m}^{i,j} = \int_{T_\ell} \int_{T_m} \frac{\varphi_{i+3}(y)\varphi_{j+3}(y)}{|x - y|^{2+2s}} \, dxdy.$$

We use two nested Gaussian quadrature rules to estimate these integrals. These have 6 quadrature nodes each, making a total of 36 quadrature points. Let us denote by p_k and w_k ($k = 1, \ldots, 6$) the quadrature nodes and weights in $\hat{T}$, respectively. Changing variables we obtain

$$A_{\ell,m}^{i,j} = 4|T_\ell||T_m| \int_{\hat{T}} \int_{\hat{T}} \frac{\hat{\varphi}_i(x)\hat{\varphi}_j(x)}{|\chi_\ell(x) - \chi_m(y)|^{2+2s}} \, dxdy,$$

and applying the quadrature rule twice, we derive:

$$(A.3) \qquad A_{\ell,m}^{i,j} \approx 4|T_\ell||T_m| \sum_{q=1}^{6} \sum_{k=1}^{6} \frac{w_q\, w_k\, \hat{\varphi}_i(p_k)\hat{\varphi}_j(p_k)}{|\chi_\ell(p_k) - \chi_m(p_q)|^{2+2s}}.$$

Note that the right hand side summands only depend on i and j through their numerators, and on ℓ and m through their denominators. As our goal is to compute the whole block $A_{\ell,m}$ as efficiently as possible, we set the following definitions:

- The matrix $\Phi^A \in \mathbb{R}^9 \times \mathbb{R}^{36}$ stores the numerators involved in (A.3), corresponding to the 9 pairs of basis functions and the 36 pairs of quadrature nodes, respectively. Namely,

$$(A.4) \qquad \Phi_{ij}^A = \hat{\varphi}_{[i-1]_3+1}(p_{\lceil \frac{j}{6} \rceil})\hat{\varphi}_{\lceil \frac{i}{3} \rceil}(p_{\lceil \frac{j}{6} \rceil})w_{[j-1]_6+1}w_{\lceil \frac{j}{6} \rceil},$$

  where $[m]_k$ denotes m modulo k and $\lceil \cdot \rceil$ is the ceiling function. Let us make this definition more explicit. The matrix Φ^A may be divided in 6 blocks,

$$\Phi^A = (\Phi^{A_1} \ldots \Phi^{A_6}),$$

  where Φ^{A_k} is a 6×9 matrix:

$$\Phi^{A_k} = \begin{pmatrix} \hat{\varphi}_1(p_k)\hat{\varphi}_1(p_k)w_kw_1 & \hat{\varphi}_1(p_k)\hat{\varphi}_1(p_k)w_kw_2 & \ldots & \hat{\varphi}_1(p_k)\hat{\varphi}_1(p_k)w_kw_6 \\ \hat{\varphi}_2(p_k)\hat{\varphi}_1(p_k)w_kw_1 & \hat{\varphi}_2(p_k)\hat{\varphi}_1(p_k)w_kw_2 & \ldots & \hat{\varphi}_2(p_k)\hat{\varphi}_1(p_k)w_kw_6 \\ \hat{\varphi}_3(p_k)\hat{\varphi}_1(p_k)w_kw_1 & \hat{\varphi}_3(p_k)\hat{\varphi}_1(p_k)w_kw_2 & \ldots & \hat{\varphi}_3(p_k)\hat{\varphi}_1(p_k)w_kw_6 \\ \hat{\varphi}_1(p_k)\hat{\varphi}_2(p_k)w_kw_1 & \hat{\varphi}_1(p_k)\hat{\varphi}_2(p_k)w_kw_2 & \ldots & \hat{\varphi}_1(p_k)\hat{\varphi}_2(p_k)w_kw_6 \\ \hat{\varphi}_2(p_k)\hat{\varphi}_2(p_k)w_kw_1 & \hat{\varphi}_2(p_k)\hat{\varphi}_2(p_k)w_kw_2 & \ldots & \hat{\varphi}_2(p_k)\hat{\varphi}_2(p_k)w_kw_6 \\ \hat{\varphi}_3(p_k)\hat{\varphi}_2(p_k)w_kw_1 & \hat{\varphi}_3(p_k)\hat{\varphi}_2(p_k)w_kw_2 & \ldots & \hat{\varphi}_3(p_k)\hat{\varphi}_2(p_k)w_kw_6 \\ \hat{\varphi}_1(p_k)\hat{\varphi}_3(p_k)w_kw_1 & \hat{\varphi}_1(p_k)\hat{\varphi}_3(p_k)w_kw_2 & \ldots & \hat{\varphi}_1(p_k)\hat{\varphi}_3(p_k)w_kw_6 \\ \hat{\varphi}_2(p_k)\hat{\varphi}_3(p_k)w_kw_1 & \hat{\varphi}_2(p_k)\hat{\varphi}_3(p_k)w_kw_2 & \ldots & \hat{\varphi}_2(p_k)\hat{\varphi}_3(p_k)w_kw_6 \\ \hat{\varphi}_3(p_k)\hat{\varphi}_3(p_k)w_kw_1 & \hat{\varphi}_3(p_k)\hat{\varphi}_3(p_k)w_kw_2 & \ldots & \hat{\varphi}_3(p_k)\hat{\varphi}_3(p_k)w_kw_6 \end{pmatrix}.$$

- The variable $d^m \in \mathbb{R}^{36}$ is a vector storing the distances between all the quadrature nodes involved:

$$(A.5) \qquad d_k^m = \left| \chi_\ell(p_{[k-1]_6+1}) - \chi_m(p_{\lceil \frac{k}{6} \rceil}) \right|^{-(2+2s)}.$$

Namely, the vector d^m can be written as:

$$d^m = \begin{pmatrix} |\chi_\ell(p_1) - \chi_m(p_1)|^{-(2+2s)} \\ \vdots \\ |\chi_\ell(p_6) - \chi_m(p_1)|^{-(2+2s)} \\ |\chi_\ell(p_1) - \chi_m(p_2)|^{-(2+2s)} \\ \vdots \\ |\chi_\ell(p_6) - \chi_m(p_2)|^{-(2+2s)} \\ \vdots \\ \vdots \\ |\chi_\ell(p_1) - \chi_m(p_6)|^{-(2+2s)} \\ \vdots \\ |\chi_\ell(p_6) - \chi_m(p_6)|^{-(2+2s)} \end{pmatrix}.$$

With these two variables in hand, the computation of the integrals A^{ij} may be done in a vectorized mode. Defining $\hat{A}_{\ell,m} := \Phi^A \cdot d^m$, we obtain:

$$A_{\ell,m}^{[i-1]_3+1,\lceil \frac{i}{3} \rceil} \approx 4|T_\ell||T_m|\hat{A}_{\ell,m}^i$$

$$= 4|T_\ell||T_m| \sum_q \sum_k w_q w_k \frac{\hat{\varphi}_{[i-1]_3+1}(p_k)\hat{\varphi}_{\lceil \frac{i}{3} \rceil}(p_k)}{|\chi_\ell(p_k) - \chi_m(p_q)|^{2+2s}}, \ i \in \{1, ..., 9\}.$$

Equivalently, using $MATLAB^{\circledR}$ notation:

$$A_{\ell,m} \approx 4|T_\ell||T_m|\texttt{reshape}(\hat{A}_{\ell,m}\texttt{, 3 , 3)}.$$

We apply the same ideas to compute the remaining blocks in (A.2). We define:

- a 9×36 matrix Φ^B, such that

$$\Phi_{ij}^B = \hat{\varphi}_{[i-1]_3+1}(p_{\lceil \frac{j}{n} \rceil})\hat{\varphi}_{\lceil \frac{i}{3} \rceil+3}(p_{[j-1]_n+1})w_{[j-1]_n+1}w_{\lceil \frac{j}{n} \rceil},$$

- a 9×36 matrix Φ^D, such that

$$\Phi_{ij}^D = \hat{\varphi}_{[i-1]_3+4}(p_{[j-1]_n+1})\hat{\varphi}_{\lceil \frac{i}{3} \rceil+3}(p_{[j-1]_n+1})w_{[j-1]_n+1}w_{\lceil \frac{j}{n} \rceil}.$$

Then, considering

$$\hat{B}_{\ell,m} := \Phi^B \cdot d^m,$$
$$\hat{D}_{\ell,m} := \Phi^D \cdot d^m,$$

we just need to multiply

$$B_{\ell,m} \approx 4|T_\ell||T_m|\texttt{reshape}(\hat{B}_{\ell,m}\texttt{, 3 , 3)},$$
$$D_{\ell,m} \approx 4|T_\ell||T_m|\texttt{reshape}(\hat{D}_{\ell,m}\texttt{, 3 , 3)}.$$

Is simple to verify that $C_{\ell,m} = B'_{\ell,m}$, so that there is no need to make additional operations to compute the block $C_{\ell,m}$. Moreover, let us emphasize that the matrices Φ^A, Φ^B and Φ^D depend on the quadrature rule employed, but not on the elements under consideration; these are precomputed and stored in `data.mat`. We refer to Section C.2 for details on how this is done. However, in the main loop, the vector d^m needs to be calculated for every $1 \le \ell \le m \le N_{\hat{\mathcal{T}}}$.

We obtain a matrix `ML` as follows:

$$\texttt{ML} \approx 4|T_\ell||T_m| \begin{pmatrix} \texttt{reshape}(\Phi^A \cdot d^m,\ 3\ ,\ 3) & \texttt{reshape}(\Phi^B \cdot d^m,\ 3\ ,\ 3) \\ \texttt{reshape}(\Phi^B \cdot d^m,\ 3\ ,\ 3)' & \texttt{reshape}(\Phi^D \cdot d^m,\ 3\ ,\ 3) \end{pmatrix}.$$

In addition, this vectorized approach gives us an efficient way to compute $I_{\ell,m}$ for several values of $m \in \{1,...,N_{\tilde{\mathcal{T}}}\}$ at once. Indeed, suppose that want to calculate $I_{\ell,m}$ for $m \in \mathcal{S} \subseteq \{1,...,N_{\tilde{\mathcal{T}}}\}$ (along the execution of the main code, $\mathcal{S}$ would contain the indices listed in `empty`). It is possible to compute $\hat{A}_{\ell,m}$, $\hat{B}_{\ell,m}$ and $\hat{D}_{\ell,m}$ for all $m \in \mathcal{S}$ using vectorized operations as follows:

$$\left(\hat{A}_{\ell,m_1}, ..., \hat{A}_{\ell,m_{\#\mathcal{S}}} \right) = \Phi^A \cdot \left(d^{m_1}, ..., d^{m_{\#\mathcal{S}}} \right),$$

$$\left(\hat{B}_{\ell,m_1}, ..., \hat{B}_{\ell,m_{\#\mathcal{S}}} \right) = \Phi^B \cdot \left(d^{m_1}, ..., d^{m_{\#\mathcal{S}}} \right),$$

$$\left(\hat{D}_{\ell,m_1}, ..., \hat{D}_{\ell,m_{\#\mathcal{S}}} \right) = \Phi^D \cdot \left(d^{m_1}, ..., d^{m_{\#\mathcal{S}}} \right).$$

Observe that, fixed ℓ and $\mathcal{S}$, the distances between interpolation points of the involved triangles are all the necessary information to obtain the estimation of the matrix `ML` (given by (A.2)), for $m \in \mathcal{S}$.

In order to perform an efficient computation of $(d^{m_1}, ..., d^{m_{\#\mathcal{S}}})$, we use the Matlab function `pdist2` in the following way:

$$(d^{m_1}, ..., d^{m_{\#\mathcal{S}}}) = \texttt{reshape}\left(\ \texttt{pdist2}(X^\ell, \begin{pmatrix} X^{m_1} \\ X^{m_2} \\ \vdots \\ X^{m_{\#\mathcal{S}}} \end{pmatrix}),\ n^2,\ \texttt{[]}\ \right)^{(-1-s)}.$$

Here, the vectors X^m are given by

$$X^m := \begin{pmatrix} \chi_m(p_1) \\ \vdots \\ \chi_m(p_6) \end{pmatrix}.$$

The computation of the matrix `ML` is carried in the main code, and it is implemented in Subsection 5.2.

A.2. **Vertex-touching elements.** In case $\overline{T_\ell} \cap \overline{T_m}$ consists of a vertex, define $\hat{z} = (\hat{x}, \hat{y})$, identify $\hat{z}$ with a vector in $\mathbb{R}^4$, and split the domain of integration in (A.1) into two components D_1 and D_2, where

$$D_1 = \{\hat{z} \colon 0 \le \hat{z}_1 \le 1,\ 0 \le \hat{z}_2 \le \hat{z}_1,\ 0 \le \hat{z}_3 \le \hat{z}_1,\ 0 \le \hat{z}_4 \le \hat{z}_3\},$$
$$D_2 = \{\hat{z} \colon 0 \le \hat{z}_3 \le 1,\ 0 \le \hat{z}_4 \le \hat{z}_3,\ 0 \le \hat{z}_1 \le \hat{z}_3,\ 0 \le \hat{z}_2 \le \hat{z}_1\}.$$

Let $\xi \in [0,1]$ and $\eta = (\eta_1, \eta_2, \eta_3) \in [0,1]^3$. We consider the mappings $T_h \colon [0,1] \times [0,1]^3 \to D_h$, $h = 1, 2$,

$$
T_1(\xi, \eta) = \begin{pmatrix} \xi \\ \xi\eta_1 \\ \xi\eta_2 \\ \xi\eta_2\eta_3 \end{pmatrix}, \quad T_2(\xi, \eta) = \begin{pmatrix} \xi\eta_2 \\ \xi\eta_2\eta_3 \\ \xi \\ \xi\eta_1 \end{pmatrix},
$$

having Jacobian determinants $|JT_1| = \xi^3\eta_2 = |JT_2|$.

We perform the calculations in detail only on D_1. Observe that if $i = 1$, which corresponds to the vertex in common between T_ℓ and T_m, then

$$
\varphi_i(\chi_\ell(\xi, \xi\eta_1)) - \varphi_i(\chi_m(\xi\eta_2, \xi\eta_2\eta_3)) = -\xi(1 - \eta_2).
$$

Meanwhile, if the subindex i equals 2 or 3, it corresponds to one of the other two vertices of T_ℓ. Therefore, in those cases $\varphi_i(\chi_m(\xi\eta_2, \xi\eta_2\eta_3)) = 0$, and

$$
\begin{aligned}
\varphi_2(\chi_\ell(\xi, \xi\eta_1)) &= \xi(1 - \eta_1), \\
\varphi_3(\chi_\ell(\xi, \xi\eta_1)) &= \xi\eta_1.
\end{aligned}
$$

Analogously, if $i \in \{4, 5\}$, then $\varphi_i(\chi_\ell(\xi, \xi\eta_1)) = 0$ and so

$$
\begin{aligned}
\varphi_4(\chi_m(\xi\eta_2, \xi\eta_2\eta_3)) &= -\xi\eta_2(1 - \eta_3), \\
\varphi_5(\chi_m(\xi\eta_2, \xi\eta_2\eta_3)) &= -\xi\eta_2\eta_3.
\end{aligned}
$$

Thus, defining the functions $\psi_k^{(1)} \colon [0,1]^3 \to \mathbb{R}$ ($k \in \{1, \dots, 5\}$),

$$
\begin{aligned}
\psi_1^{(1)}(\eta) &= \eta_2 - 1, & \psi_2^{(1)}(\eta) &= 1 - \eta_1, & \psi_3^{(1)}(\eta) &= \eta_1, \\
\psi_4^{(1)}(\eta) &= -\eta_2(1 - \eta_3), & \psi_5^{(1)}(\eta) &= -\eta_2\eta_3,
\end{aligned}
$$

we may write

$$
\begin{aligned}
\int_{D_1} F_{ij}(\hat{z}) \, d\hat{z} &= \int_{[0,1]} \int_{[0,1]^3} \frac{\psi_i^{(1)}(\eta)\psi_j^{(1)}(\eta)}{\left| B_\ell \begin{pmatrix} \xi \\ \xi\eta_1 \end{pmatrix} - B_m \begin{pmatrix} \xi\eta_2 \\ \xi\eta_2\eta_3 \end{pmatrix} \right|^{2+2s}} \xi^5\eta_2 \, d\eta \, d\xi \\
&= \left(\int_0^1 \xi^{3-2s} d\xi \right) \left(\int_{[0,1]^3} \frac{\psi_i^{(1)}(\eta)\psi_j^{(1)}(\eta)}{\left| d^{(1)}(\eta) \right|^{2+2s}} \eta_2 \, d\eta \right) \\
&= \frac{1}{4 - 2s} \left(\int_{[0,1]^3} \frac{\psi_i^{(1)}(\eta)\psi_j^{(1)}(\eta)}{\left| d^{(1)}(\eta) \right|^{2+2s}} \eta_2 \, d\eta \right),
\end{aligned}
$$

where we have defined the function

$$
d^{(1)}(\eta) = B_\ell \begin{pmatrix} 1 \\ \eta_1 \end{pmatrix} - B_m \begin{pmatrix} \eta_2 \\ \eta_2\eta_3 \end{pmatrix}.
$$

Observe that in the first line of last equation (or equivalently, in (A.1)), the integrand is singular at the origin. The key point in the identity above is that the singularity of the integral is explicitly computed. The function $d^{(1)}$ is not zero on $[0,1]^3$, and therefore the last integral involves a regular integrand that is easily estimated by means of a Gaussian quadrature rule.

In a similar fashion, the integrals over D_2 take the form

$$\int_{D_2} F_{ij}(\hat{z})\,d\hat{z} = \frac{1}{4-2s}\left(\int_{[0,1]^3} \frac{\psi_i^{(2)}(\eta)\psi_j^{(2)}(\eta)}{\left|d^{(2)}(\eta)\right|^{2+2s}}\,\eta_2\,d\eta\right),$$

where

$$\psi_1^{(2)}(\eta) = 1 - \eta_2, \qquad \psi_2^{(2)}(\eta) = \eta_2(1-\eta_3), \qquad \psi_3^{(2)}(\eta) = \eta_2\eta_3,$$
$$\psi_4^{(2)}(\eta) = \eta_1 - 1, \qquad \psi_5^{(2)}(\eta) = -\eta_1,$$

and

$$d^{(2)}(\eta) = B_\ell\begin{pmatrix} \eta_2 \\ \eta_2\eta_3 \end{pmatrix} - B_m\begin{pmatrix} 1 \\ \eta_1 \end{pmatrix}.$$

Based on the previous analysis, we describe the function `vertex_quad`. Let $p_1, ..., p_n \in [0,1]^3$ be a set of quadrature points and $w_1, ..., w_n$ their respective weights. In the code we present, we work with three nested three-point quadrature rules on $[0,1]$, making a total of 27 quadrature nodes in the unit cube. The data necessary to use this quadrature is supplied in the file `data.mat`, and in Appendix C.1.

Set $h \in \{1,2\}$. Then, applying the mentioned quadrature rule in the cube,

$$\int_{[0,1]^3} \frac{\psi_i^{(h)}(\eta)\psi_j^{(h)}(\eta)}{\left|d^{(h)}(\eta)\right|^{2+2s}}\,\eta_2\,d\eta \approx \sum_{k=1}^{27} w_k \frac{\psi_i^{(h)}(p_k)\psi_j^{(h)}(p_k)}{\left|d^{(h)}(p_k)\right|^{2+2s}}\,p_{k,2},$$

where $p_{k,2}$ denotes the second coordinate of the point p_k. The right hand side only depends on ℓ and m through $d^{(h)}$. So, in order to compute $I_{\ell,m}^{i,j}$ using vectorized operations, we define the following variables, in analogy to (A.4) and (A.5):

- A 25×27 matrix Ψ^h satisfying

$$\Psi_{ij}^h = w_j\,\psi_{[i-1]_5+1}^{(h)}(p_j)\psi_{\lceil \frac{i}{5}\rceil}^{(h)}(p_j)\,p_{j,2}.$$

- A vector $d^h \in \mathbb{R}^{27}$, such that

$$d_k^h = \left|d^{(h)}(p_k)\right|^{2+2s}.$$

Then, defining $\hat{I}_{\ell,m} := \Psi^1 \cdot d^1 + \Psi^2 \cdot d^2$, we obtain

$$I_{\ell,m}^{[i-1]_5+1,\lceil \frac{i}{5}\rceil} \approx \frac{4|T_\ell||T_m|}{4-2s}\hat{I}_{\ell,m}^i$$
$$= \sum_{h=1}^{2}\sum_{k=1}^{27} w_k \frac{\psi_{[i-1]_5+1}^{(h)}(p_k)\psi_{\lceil \frac{i}{5}\rceil}^{(h)}(p_k)}{\left|d^{(h)}(p_k)\right|^{2+2s}}, \quad i \in \{1, ..., 25\}.$$

Equivalently, using $MATLAB^{\circledR}$ notation:

$$I_{\ell,m} \approx \frac{4|T_\ell||T_m|}{4-2s}\texttt{reshape}(\hat{I}_{\ell,m},\ 5\ ,\ 5).$$

Given that the matrices Ψ^1 and Ψ^2 do not change along the execution, we only need to compute them once. These are precomputed and provided on the data file; explicit information regarding its entries is available on Appendix C.3.

So, the function `vertex_quad` computes the previous quadrature rule in the following way:

```
function ML = vertex_quad (nodl,nodm,sh_nod,p,s,psi1,psi2,areal,aream,p_c)
xm = p(1, nodm);
ym = p(2, nodm);
xl = p(1, nodl);
yl = p(2, nodl);
x = p_c(:,1);
y = p_c(:,2);
z = p_c(:,3);
local_l = find(nodl==sh_nod);
nsh_l = find(nodl~=sh_nod);
nsh_m = find(nodm~=sh_nod);
p_c = [xl(local_l), yl(local_l)];
Bl = [xl(nsh_l(1))-p_c(1) xl(nsh_l(2))-xl(nsh_l(1));
      yl(nsh_l(1))-p_c(2) yl(nsh_l(2))-yl(nsh_l(1))];
Bm = [xm(nsh_m(1))-p_c(1) xm(nsh_m(2))-xm(nsh_m(1));
      ym(nsh_m(1))-p_c(2) ym(nsh_m(2))-ym(nsh_m(1))];
ML = ( 4*areal*aream/(4-2*s) ).*reshape(...
    psi1*( sum( ([ones(length(x),1)  x]*(Bl')...
            - [y , y.*z]*(Bm') ).^2, 2 ).^(-1-s) ) +...
    psi2*( sum( ([ones(length(x),1)  x]*(Bm')...
            - [y , y.*z]*(Bl') ).^2, 2 ).^(-1-s) )...
    , 5 , 5);
end
```

In the code above, `nodl` and `nodm` are the vertex indices of T_ℓ and T_m respectively, `sh_nod` is the index of the shared node, `p` is an array that contains all the vertex coordinates, `areal` and `aream` denote $|T_\ell|$ and $|T_m|$ respectively, `s` is s, and `p_c` contains the coordinates of the quadrature points on $[0,1]^3$. This last variable is gathered form `data.mat`, where it is stored as `p_cube` (see Appendix C.1). In addition, `Bl` and `Bm` play the role of B_ℓ and B_m, and `psi1` and `psi2` are Ψ^1 and Ψ^2 respectively. As we mentioned, `psi1` and `psi2` have been pre-computed and stored on `data.mat` as `vpsi1` and `vpsi2` respectively (see Appendix C.3).

The output of `vertex_quad` is a 6×6 matrix `ML` that satisfies `ML(i,j)` $\approx I_{\ell,m}^{i,j}$.

A.3. **Edge-touching elements.** In this case, the parametrization of the elements we are considering is such that both χ_ℓ and χ_m map $[0,1] \times \{0\}$ to the common edge between T_ℓ and T_m. Therefore, if we consider $\hat{z} = (\hat{y}_1 - \hat{x}_1, \hat{y}_2, \hat{x}_2)$, the singularity of the integrand is localized at $\hat{z} = 0$:

$$I_{\ell,m}^{i,j} = 4|T_\ell||T_m| \int_0^1 \int_{-\hat{x}_1}^{1-\hat{x}_1} \int_0^{\hat{z}_1+\hat{x}_1} \int_0^{\hat{x}_1} F_{ij}(\hat{x}_1, \hat{z}_3, \hat{x}_1 + \hat{z}_1, \hat{z}_2) \, d\hat{z} \, d\hat{x}_1.$$

We decompose the domain of integration as $\cup_{k=1}^5 D_k$, where

$$D_1 = \{(\hat{x}_1, \hat{z}) : -1 \le \hat{z}_1 \le 0, \, 0 \le \hat{z}_2 \le 1 + \hat{z}_1,$$
$$0 \le \hat{z}_3 \le \hat{z}_2 - \hat{z}_1, \, \hat{z}_2 - \hat{z}_1 \le \hat{x}_1 \le 1\},$$
$$D_2 = \{(\hat{x}_1, \hat{z}) : -1 \le \hat{z}_1 \le 0, \, 0 \le \hat{z}_2 \le 1 + \hat{z}_1,$$
$$\hat{z}_2 - \hat{z}_1 \le \hat{z}_3 \le 1, \, \hat{z}_3 \le \hat{x}_1 \le 1\},$$
$$D_3 = \{(\hat{x}_1, \hat{z}) : 0 \le \hat{z}_1 \le 1, \, 0 \le \hat{z}_2 \le \hat{z}_1,$$

$$0 \le \hat{z}_3 \le 1 - \hat{z}_1, \ \hat{z}_3 \le \hat{x}_1 \le 1 - \hat{z}_1\},$$

$$D_4 = \{(\hat{x}_1, \hat{z}) \colon 0 \le \hat{z}_1 \le 1, \ \hat{z}_1 \le \hat{z}_2 \le 1,$$
$$0 \le \hat{z}_3 \le \hat{z}_2 - \hat{z}_1, \ \hat{z}_2 - \hat{z}_1 \le \hat{x}_1 \le 1 - \hat{z}_1\},$$

$$D_5 = \{(\hat{x}_1, \hat{z}) \colon 0 \le \hat{z}_1 \le 1, \ \hat{z}_1 \le \hat{z}_2 \le 1,$$
$$\hat{z}_2 - \hat{z}_1 \le \hat{z}_3 \le 1 - \hat{z}_1, \ \hat{z}_3 \le \hat{x}_1 \le 1 - \hat{z}_1\}.$$

Consider the mappings $T_k \colon [0,1] \times [0,1]^3 \to D_k \ (k \in \{1, \ldots, 5\})$,

$$T_1\begin{pmatrix} \xi \\ \eta \end{pmatrix} = \begin{pmatrix} \xi \\ -\xi\eta_1\eta_2 \\ \xi\eta_1(1-\eta_2) \\ \xi\eta_1\eta_3 \end{pmatrix}, \qquad T_2\begin{pmatrix} \xi \\ \eta \end{pmatrix} = \begin{pmatrix} \xi \\ -\xi\eta_1\eta_2\eta_3 \\ \xi\eta_1\eta_2(1-\eta_3) \\ \xi\eta_1 \end{pmatrix},$$

$$T_3\begin{pmatrix} \xi \\ \eta \end{pmatrix} = \begin{pmatrix} \xi(1-\eta_1\eta_2) \\ \xi\eta_1\eta_2 \\ \xi\eta_1\eta_2\eta_3 \\ \xi\eta_1(1-\eta_2) \end{pmatrix}, \qquad T_4\begin{pmatrix} \xi \\ \eta \end{pmatrix} = \begin{pmatrix} \xi(1-\eta_1\eta_2\eta_3) \\ \xi\eta_1\eta_2\eta_3 \\ \xi\eta_1 \\ \xi\eta_1\eta_2(1-\eta_3) \end{pmatrix},$$

$$T_5\begin{pmatrix} \xi \\ \eta \end{pmatrix} = \begin{pmatrix} \xi(1-\eta_1\eta_2\eta_3) \\ \xi\eta_1\eta_2\eta_3 \\ \xi\eta_1\eta_2 \\ \xi\eta_1(1-\eta_2\eta_3) \end{pmatrix},$$

with Jacobian determinants given by

$$|JT_1| = \xi^3\eta_1^2, \quad |JT_h| = \xi^3\eta_1^2\eta_2, \ h \in \{2, \ldots, 5\}.$$

Then, over D_h it holds that

$$\int_{D_h} F_{ij} = \frac{1}{4-2s} \int_{[0,1]^3} \frac{\psi_i^{(h)}(\eta)\psi_j^{(h)}(\eta)}{|d^{(h)}(\eta)|^{2+2s}} J^{(h)}(\eta)\, d\eta,$$

where

$$\psi_1^{(1)}(\eta) = -\eta_1\eta_2, \qquad \psi_2^{(1)}(\eta) = \eta_1(1-\eta_3),$$
$$\psi_3^{(1)}(\eta) = \eta_1\eta_3, \qquad \psi_4^{(1)}(\eta) = -\eta_1(1-\eta_2),$$
$$\psi_1^{(2)}(\eta) = -\eta_1\eta_2\eta_3, \qquad \psi_2^{(2)}(\eta) = -\eta_1(1-\eta_2),$$
$$\psi_3^{(2)}(\eta) = \eta_1, \qquad \psi_4^{(2)}(\eta) = -\eta_1\eta_2(1-\eta_3),$$
$$\psi_1^{(3)}(\eta) = \eta_1\eta_2, \qquad \psi_2^{(3)}(\eta) = -\eta_1(1-\eta_2\eta_3),$$
$$\psi_3^{(3)}(\eta) = \eta_1(1-\eta_2), \qquad \psi_4^{(3)}(\eta) = -\eta_1\eta_2\eta_3,$$
$$\psi_1^{(4)}(\eta) = \eta_1\eta_2\eta_3, \qquad \psi_2^{(4)}(\eta) = \eta_1(1-\eta_2),$$
$$\psi_3^{(4)}(\eta) = \eta_1\eta_2(1-\eta_3), \qquad \psi_4^{(4)}(\eta) = -\eta_1,$$
$$\psi_1^{(5)}(\eta) = \eta_1\eta_2\eta_3, \qquad \psi_2^{(5)}(\eta) = -\eta_1(1-\eta_2),$$
$$\psi_3^{(5)}(\eta) = \eta_1(1-\eta_2\eta_3), \qquad \psi_4^{(5)}(\eta) = -\eta_1\eta_2.$$

Moreover, the functions $d^{(h)}$ are given by

$$d^{(1)}(\eta) = B_\ell\begin{pmatrix} 1 \\ \eta_1\eta_3 \end{pmatrix} - B_m\begin{pmatrix} 1-\eta_1\eta_2 \\ \eta_1(1-\eta_2) \end{pmatrix},$$

$$d^{(2)}(\eta) = B_\ell \begin{pmatrix} 1 \\ \eta_1 \end{pmatrix} - B_m \begin{pmatrix} 1 - \eta_1\eta_2\eta_3 \\ \eta_1\eta_2(1-\eta_3) \end{pmatrix},$$

$$d^{(3)}(\eta) = B_\ell \begin{pmatrix} 1 - \eta_1\eta_2 \\ \eta_1(1-\eta_2) \end{pmatrix} - B_m \begin{pmatrix} 1 \\ \eta_1\eta_2\eta_3 \end{pmatrix},$$

$$d^{(4)}(\eta) = B_\ell \begin{pmatrix} 1 - \eta_1\eta_2\eta_3 \\ \eta_1\eta_2(1-\eta_3) \end{pmatrix} - B_m \begin{pmatrix} 1 \\ \eta_1 \end{pmatrix},$$

$$d^{(5)}(\eta) = B_\ell \begin{pmatrix} 1 - \eta_1\eta_2\eta_3 \\ \eta_1(1-\eta_2\eta_3) \end{pmatrix} - B_m \begin{pmatrix} 1 \\ \eta_1\eta_2 \end{pmatrix},$$

and the Jacobians are

$$J^{(1)}(\eta) = \eta_1^2, \quad J^{(h)}(\eta) = \eta_1^2\eta_2, \ h \in \{2,\dots,5\}.$$

As in the case of vertex-touching elements, the problem is reduced to computing integrals on the unit cube. Let $p_1,...,p_{27} \in [0,1]^3$ the quadrature points, and $w_1,...,w_{27}$ their respective weights. For $h = 1,\dots,5$ we have

$$\int_{[0,1]^3} \frac{\psi_i^{(h)}(\eta)\psi_j^{(h)}(\eta)}{\left|d^{(h)}(\eta)\right|^{2+2s}} J^{(h)}(\eta)\, d\eta \approx \sum_k w_k \frac{\psi_i^{(h)}(p_k)\psi_j^{(h)}(p_k)}{\left|d^{(h)}(p_k)\right|^{2+2s}} J^{(h)}(p_k).$$

Once more, the right hand side only depends on ℓ and m through $d^{(h)}$. So, with the purpose of computing $I_{\ell,m}$ efficiently, we define:

- A matrix $\Psi^h \in \mathbb{R}^{16\times 27}$, given by
$$\Psi_{ij}^h = w_j\, \psi_{[i-1]_4+1}(p_j)\psi_{\lceil\frac{i}{4}\rceil}(p_j)J^{(h)}(p_j).$$

- A vector $d^h \in \mathbb{R}^{27}$, such that
$$d_k^h = \left|d^{(h)}(p_k)\right|^{2+2s}.$$

Therefore, considering $\hat{I}_{\ell,m} = \Psi^1 \cdot d^1 + \cdots + \Psi^5 \cdot d^5$, we reach the following relation:

$$I_{\ell,m}^{[i-1]_4+1,\lceil\frac{i}{4}\rceil} \approx \frac{4|T_\ell||T_m|}{4-2s}\hat{I}_{\ell,m}^i$$

$$= \sum_h \sum_k w_k \frac{\psi_{[i-1]_4+1}^{(h)}(p_k)\psi_{\lceil\frac{i}{4}\rceil}^{(h)}(p_k)}{\left|d^{(h)}(p_k)\right|^{2+2s}}, \ i \in \{1,...,16\}.$$

Using $MATLAB^{\circledR}$ notation,

$$I_{\ell,m} \approx \frac{4|T_\ell||T_m|}{4-2s}\texttt{reshape}(\hat{I}_{\ell,m},\ \texttt{4}\ ,\ \texttt{4}).$$

As before, the matrices Ψ^1, $\dots$, Ψ^5 do not depend on the elements under consideration, so they are precomputed and provided in `data.mat`, where they are stored as `epsi1,...,epsi5`, respectively. Details about their calculation are given in Appendix C.4.

The function `edge_quad` performs the calculations we have explained in this section.

```
function ML = edge_quad(nodl,nodm,nod_diff,p,s,psi1,psi2,psi3,...
                        psi4,psi5,areal,aream,p_c)
xm = p(1, nodm);
ym = p(2, nodm);
```

```
xl = p(1, nodl);
yl = p(2, nodl);
x = p_c(:,1);
y = p_c(:,2);
z = p_c(:,3);
local_l = find(nodl~=nod_diff(1));
nsh_l = find(nodl==nod_diff(1));
nsh_m = find(nodm==nod_diff(2));
P1 = [xl(local_l(1)), yl(local_l(1))];
P2 = [xl(local_l(2)), yl(local_l(2))];
Bl = [P2(1)-P1(1) -P2(1)+xl(nsh_l);
      P2(2)-P1(2) -P2(2)+yl(nsh_l)];
Bm = [P2(1)-P1(1) -P2(1)+xm(nsh_m);
      P2(2)-P1(2) -P2(2)+ym(nsh_m)];
ML = ( 4*areal*aream/(4-2*s) ).*reshape(...
      psi1*( sum( ([ones(length(x),1)  x.*z]*(Bl')...
          - [1-x.*y  x.*(1-y)]*(Bm') ).^2, 2 ).^(-1-s) ) +...
      psi2*( sum( ([ones(length(x),1)  x]*(Bl')...
          - [1-x.*y.*z  x.*y.*(1-z)]*(Bm') ).^2, 2 ).^(-1-s) ) +...
      psi3*( sum( ([(1-x.*y)  x.*(1-y)]*(Bl')...
          - [ones(length(x),1) x.*y.*z]*(Bm') ).^2, 2 ).^(-1-s) ) +...
      psi4*( sum( ([1-x.*y.*z  x.*y.*(1-z)]*(Bl')...
          - [ones(length(x),1) x]*(Bm') ).^2, 2 ).^(-1-s) ) +...
      psi5*( sum( ([1-x.*y.*z  x.*(1-y.*z)]*(Bl')...
          - [ones(length(x),1) x.*y]*(Bm') ).^2, 2 ).^(-1-s) )...
      , 4 , 4);
end
```

Here, `nodl` and `nodm` are the indices of the vertices of T_ℓ and T_m respectively, `nod_diff` contains the not-shared-vertex index, `p` is an array that contains all the vertex coordinates, `areal` and `aream` are $|T_\ell|$ and $|T_m|$ respectively, `s` is s, `p_c` contains the coordinates of the quadrature points on $[0,1]^3$ (stored in `data.mat`, see Appendix C.1), `Bl` and `Bm` are B_ℓ and B_m, and `psi1`, ..., `psi5` are $\Psi^1, \ldots, \Psi^5$ respectively.

The output of this function is a 4×4 matrix `ML` $\approx I_{\ell,m}$.

A.4. **Identical elements.** In the same spirit as before, let us consider $\hat{z} = \hat{y} - \hat{x}$, so that

$$
I_{\ell,\ell} = 4|T_\ell|^2 \int_0^1 \int_0^{\hat{x}_1} \int_{-\hat{x}_1}^{1-\hat{x}_1} \int_{-\hat{x}_2}^{\hat{z}_1+\hat{x}_1-\hat{x}_2} F_{ij}(\hat{x}_1, \hat{x}_2, \hat{x}_1 + \hat{z}_1, \hat{x}_2 + \hat{z}_2)\, d\hat{z}_2\, d\hat{z}_1\, d\hat{x}_2\, d\hat{x}_1.
$$

Let us decompose the integration region into

$$
\begin{aligned}
D_1 = \{(\hat{x}, \hat{z})\colon &-1 \leq \hat{z}_1 \leq 0, \ -1 \leq \hat{z}_2 \leq \hat{z}_1, \\
&- \hat{z}_2 \leq \hat{x}_1 \leq 1, \ -\hat{z}_2 \leq \hat{x}_2 \leq \hat{x}_1\}, \\
D_2 = \{(\hat{x}, \hat{z})\colon &0 \leq \hat{z}_1 \leq 1, \ \hat{z}_1 \leq \hat{z}_2 \leq 1, \\
&\hat{z}_2 - \hat{z}_1 \leq \hat{x}_1 \leq 1 - \hat{z}_1, \ 0 \leq \hat{x}_2 \leq \hat{z}_1 - \hat{z}_2 + \hat{x}_1\}, \\
D_3 = \{(\hat{x}, \hat{z})\colon &-1 \leq \hat{z}_1 \leq 0, \ \hat{z}_1 \leq \hat{z}_2 \leq 0, \\
&- \hat{z}_1 \leq \hat{x}_1 \leq 1, \ -\hat{z}_2 \leq \hat{x}_2 \leq \hat{x}_1 + \hat{z}_1 - \hat{z}_2\}, \\
D_4 = \{(\hat{x}, \hat{z})\colon &0 \leq \hat{z}_1 \leq 1, \ 0 \leq \hat{z}_2 \leq \hat{z}_1, \\
&0 \leq \hat{x}_1 \leq 1 - \hat{z}_1, \ 0 \leq \hat{x}_2 \leq \hat{x}_1\}, \\
D_5 = \{(\hat{x}, \hat{z})\colon &-1 \leq \hat{z}_1 \leq 0, \ 0 \leq \hat{z}_2 \leq 1 + \hat{z}_1, \\
&\hat{z}_2 - \hat{z}_1 \leq \hat{x}_1 \leq 1, \ 0 \leq \hat{x}_2 \leq \hat{x}_1 + \hat{z}_1 - \hat{z}_2\}, \\
D_6 = \{(\hat{x}, \hat{z})\colon &0 \leq \hat{z}_1 \leq 1, \ -1 + \hat{z}_1 \leq \hat{z}_2 \leq 0, \\
&- \hat{z}_2 \leq \hat{x}_1 \leq 1 - \hat{z}_1, \ -\hat{z}_2 \leq \hat{x}_2 \leq \hat{x}_1\}.
\end{aligned}
$$
(A.6)

We begin by considering the first two sets. Making the change of variables $(\hat{x}', \hat{z}') = (\hat{x}, -\hat{z})$ on D_1 and $(\hat{x}', \hat{z}') = (\hat{x} + \hat{z}, \hat{z})$ on D_2, both regions are transformed into

$$
D_1' = \{(\hat{x}', \hat{z}')\colon 0 \leq \hat{z}_1' \leq 1, \ \hat{z}_1' \leq \hat{z}_2' \leq 1, \ \hat{z}_2' \leq \hat{x}_1' \leq 1, \ \hat{z}_2' \leq \hat{x}_2' \leq \hat{x}_1'\},
$$

so that

$$
4|T_\ell|^2 \int_{D_1 \cup D_2} F_{ij}(\hat{x}, \hat{x} + \hat{z}) = 4|T_\ell|^2 \int_{D_1'} F_{ij}(\hat{x}', \hat{x}' - \hat{z}') + F_{ij}(\hat{x}' - \hat{z}', \hat{x}') \, d\hat{x}' \, d\hat{z}'
$$
$$
= 8|T_\ell|^2 \int_{D_1'} F_{ij}(\hat{x}', \hat{x}' - \hat{z}') \, d\hat{x}' \, d\hat{z}',
$$

because

$$
F_{ij}(\hat{x}', \hat{x}' - \hat{z}') = \frac{(\hat{\varphi}_i(\hat{x}') - \hat{\varphi}_i(\hat{x}' - \hat{z}'))(\hat{\varphi}_j(\hat{x}') - \hat{\varphi}_j(\hat{x}' - \hat{z}'))}{|B_\ell(\hat{z}')|^{2+2s}} = F_{ij}(\hat{x}' - \hat{z}', \hat{x}').
$$

Next, consider the four-dimensional simplex

$$
D = \{w\colon 0 \leq w_1 \leq 1, \ 0 \leq w_2 \leq w_1, \ 0 \leq w_3 \leq w_2, \ 0 \leq w_4 \leq w_3\},
$$

the map $T_1 \colon D \to D_1'$,

$$
\begin{pmatrix} \hat{x}' \\ \hat{z}' \end{pmatrix} = T_1 \begin{pmatrix} w_1 \\ w_2 \\ w_3 \\ w_4 \end{pmatrix} = \begin{pmatrix} w_1, \\ w_1 - w_2 + w_3, \\ w_4, \\ w_3 \end{pmatrix}, \quad |JT_1| = 1,
$$

and the Duffy-type transform $T \colon [0,1]^4 \to D$,

(A.7)
$$
w = T \begin{pmatrix} \xi \\ \eta \end{pmatrix} = \begin{pmatrix} \xi, \\ \xi \eta_1, \\ \xi \eta_1 \eta_2, \\ \xi \eta_1 \eta_2 \eta_3 \end{pmatrix}, \quad |JT| = \xi^3 \eta_1^2 \eta_2.
$$

The composition of these two changes of variables allows to write the variables in F_{ij} in terms of (ξ, η) in the following way:

$$\hat{x}' = \left(\begin{array}{c} \xi \\ \xi(1 - \eta_1 + \eta_1\eta_2) \end{array} \right), \ \hat{z}' = \left(\begin{array}{c} \xi\eta_1\eta_2\eta_3 \\ \xi\eta_1\eta_2 \end{array} \right), \ \hat{x} - \hat{z}' = \left(\begin{array}{c} \xi(1 - \eta_1\eta_2\eta_3) \\ \xi(1 - \eta_1) \end{array} \right).$$

Observe that

$$\Lambda_k^{(1)}(\xi, \eta) := \hat{\varphi}_k(\hat{x}') - \hat{\varphi}_k(\hat{x}' - \hat{z}') = \begin{cases} -\xi\eta_1\eta_2\eta_3 & \text{if } k = 1, \\ -\xi\eta_1\eta_2(1 - \eta_3) & \text{if } k = 2, \\ \xi\eta_1\eta_2 & \text{if } k = 3. \end{cases}$$

Thus,

$$4|T_\ell|^2 \int_{D_1 \cup D_2} F_{ij}(\hat{x}, \hat{x} + \hat{z}) = 8|T_\ell|^2 \int_D F_{ij}(w_1, w_1 - w_2 + w_3, w_4, w_3)\, dw =$$

$$= 8|T_\ell|^2 \int_{[0,1]^4} \frac{\Lambda_i^{(1)}(\xi, \eta)\, \Lambda_j^{(1)}(\xi, \eta)}{\left| B_\ell \left(\begin{array}{c} \xi\eta_1\eta_2\eta_3 \\ \xi\eta_1\eta_2 \end{array} \right) \right|^{2+2s}} \xi^3 \eta_1^2 \eta_2\, d\xi\, d\eta.$$

Finally, as the functions $\Lambda_k^{(1)}$ may be rewritten as $\Lambda_k^{(1)}(\xi, \eta) = \xi\eta_1\eta_2\psi_k^{(1)}(\eta_3)$, where

$$\psi_1^{(1)}(\eta_3) = -\eta_3, \quad \psi_2^{(1)}(\eta_3) = -(1 - \eta_3), \quad \psi_3^{(1)}(\eta_3) = 1,$$

we obtain

$$4|T_\ell|^2 \int_{D_1 \cup D_2} F_{ij}(\hat{x}, \hat{x} + \hat{z}) =$$

$$= 8|T_\ell|^2 \int_0^1 \xi^{3-2s} d\xi \int_0^1 \eta_1^{2-2s} d\eta_1 \int_0^1 \eta_2^{1-2s} d\eta_2 \int_0^1 \frac{\psi_i^{(1)}(\eta_3)\psi_j^{(1)}(\eta_3)}{\left| B_\ell \left(\begin{array}{c} \eta_3 \\ 1 \end{array} \right) \right|^{2+2s}} d\eta_3.$$

Obviously, the first three integrals above are straightforwardly calculated by hand, and the last one involves a regular integrand, so that it is easily estimated by means of a Gaussian quadrature rule.

It still remains to perform similar calculations on the rest of the sets in (A.6). Consider the new variables $(\hat{x}', \hat{z}') = (\hat{x}, -\hat{z})$ on D_3, $(\hat{x}', \hat{z}') = (\hat{x} + \hat{z}, \hat{z})$ on D_4, $(\hat{x}', \hat{z}') = (\hat{x} + \hat{z}, \hat{z})$ on D_5 and $(\hat{x}', \hat{z}') = (\hat{x}, -\hat{z})$ on D_6, so that

$$4|T_\ell|^2 \int_{D_3 \cup D_4} F_{ij}(\hat{x}, \hat{x} + \hat{z}) = 8|T_\ell|^2 \int_{D_2'} F_{ij}(\hat{x}', \hat{x}' - \hat{z}')\, d\hat{x}'\, d\hat{z}',$$

$$4|T_\ell|^2 \int_{D_5 \cup D_6} F_{ij}(\hat{x}, \hat{x} + \hat{z}) = 8|T_\ell|^2 \int_{D_3'} F_{ij}(\hat{x}', \hat{x}' - \hat{z}')\, d\hat{x}'\, d\hat{z}',$$

where

$$D_2' = \{(\hat{x}', \hat{z}')\colon 0 \le \hat{z}_1' \le 1,\ 0 \le \hat{z}_2' \le \hat{z}_1',\ \hat{z}_1' \le \hat{x}_1' \le 1,\ \hat{z}_2' \le \hat{x}_2' \le \hat{x}_1' - \hat{z}_1' + \hat{z}_2'\},$$

$$D_3' = \{(\hat{x}', \hat{z}')\colon -1 \le \hat{z}_1' \le 0,\ 0 \le \hat{z}_2' \le 1 + \hat{z}_1',\ \hat{z}_2' \le \hat{x}_1' \le 1 + \hat{z}_1',\ \hat{z}_2' \le \hat{x}_2' \le \hat{x}_1'\}.$$

These domains are transformed into $[0,1]^4$ by the respective composition of the transformations $T_h \colon D \to D'_h$ $(h = 1, 2)$

$$T_2 \begin{pmatrix} w_1 \\ w_2 \\ w_3 \\ w_4 \end{pmatrix} = \begin{pmatrix} w_1 \\ w_2 - w_3 + w_4 \\ w_3 \\ w_4 \end{pmatrix}, \quad T_3 \begin{pmatrix} w_1 \\ w_2 \\ w_3 \\ w_4 \end{pmatrix} = \begin{pmatrix} w_1 - w_4 \\ w_2 - w_4 \\ -w_4 \\ w_3 - w_4 \end{pmatrix},$$

and the Duffy transformation (A.7). Simple calculations lead finally to

$$4|T_\ell|^2 \int_{D_3 \cup D_4} F_{ij}(\hat{x}, \hat{x} + \hat{z}) = \frac{8|T_\ell|^2}{(4 - 2s)(3 - 2s)(2 - 2s)} \int_0^1 \frac{\psi_i^{(2)}(\eta_3)\psi_j^{(2)}(\eta_3)}{\left| B_\ell \begin{pmatrix} 1 \\ \eta_3 \end{pmatrix} \right|^{2+2s}} d\eta_3,$$

$$4|T_\ell|^2 \int_{D_5 \cup D_6} F_{ij}(\hat{x}, \hat{x} + \hat{z}) = \frac{8|T_\ell|^2}{(4 - 2s)(3 - 2s)(2 - 2s)} \int_0^1 \frac{\psi_i^{(3)}(\eta_3)\psi_j^{(3)}(\eta_3)}{\left| B_\ell \begin{pmatrix} \eta_3 \\ 1 - \eta_3 \end{pmatrix} \right|^{2+2s}} d\eta_3,$$

where

$$\psi_1^{(2)}(\eta_3) = -1, \qquad \psi_2^{(2)}(\eta_3) = 1 - \eta_3, \qquad \psi_3^{(2)}(\eta_3) = \eta_3,$$
$$\psi_1^{(3)}(\eta_3) = \eta_3, \qquad \psi_2^{(3)}(\eta_3) = -1, \qquad \psi_3^{(3)}(\eta_3) = 1 - \eta_3.$$

For the sake of simplicity of notation, we write

$$d^{(1)}(x) := \left| B_\ell \begin{pmatrix} x \\ 1 \end{pmatrix} \right|^{2+2s}, \qquad d^{(2)}(x) := \left| B_\ell \begin{pmatrix} 1 \\ x \end{pmatrix} \right|^{2+2s},$$

$$d^{(3)}(x) := \left| B_\ell \begin{pmatrix} x \\ 1 - x \end{pmatrix} \right|^{2+2s}.$$

In order to estimate the integrals in the unit interval, we use a 9 point Gaussian quadrature rule. Let $p_1, \dots, p_9 \in [0, 1]$ the quadrature points, and $w_1, \dots, w_9$ their respective weights. Considering the integrals over the domains D'_h $(h \in \{1, 2, 3\})$, we may write

$$\int_0^1 \frac{\psi_i^{(h)}(\eta)\psi_j^{(h)}(\eta)}{d^{(h)}(\eta)} d\eta \approx \sum_{k=1}^9 w_k \frac{\psi_i^{(h)}(p_k)\psi_j^{(h)}(p_k)}{d^{(h)}(p_k)}.$$

As before, we take advantage of the fact that the integrand only depends on ℓ through its denominator. We define:

- A 9×9 matrix Ψ^h, such that

$$\Psi_{ij}^h = w_j \, \psi_{[i-1]_3+1}(p_j)\psi_{\lceil \frac{i}{3} \rceil}(p_j) \, J^{(h)}(p_j).$$

- A vector $d^h \in \mathbb{R}^9$, given by

$$d_k^h = d^{(h)}(p_k).$$

Setting $\hat{I}_{\ell,m} := \Psi^1 \cdot d^1 + \Psi^2 \cdot d^2 + \Psi^3 \cdot d^3$, we obtain, for $i \in \{1, \dots, 9\}$,

$$I_{\ell,m}^{[i-1]_3+1, \lceil \frac{i}{3} \rceil} \approx \frac{8|T_\ell|^2}{(4 - 2s)(3 - 2s)(2 - 2s)} \hat{I}_{\ell,m}^i$$

$$= \frac{8|T_\ell|^2}{(4-2s)(3-2s)(2-2s)} \sum_{h=1}^{3} \sum_{k=1}^{9} w_k \frac{\psi_{[i-1]_3+1}^{(h)}(p_k) \psi_{\lceil \frac{i}{3} \rceil}^{(h)}(p_k)}{d^{(h)}(p_k)},$$

or in *MATLAB*® notation,

$$I_{\ell,m} \approx \frac{8|T_\ell|^2}{(4-2s)(3-2s)(2-2s)} \, \texttt{reshape}(\hat{I}_{\ell,m}, \texttt{3}, \texttt{3}).$$

The matrices Ψ^1, Ψ^2 and Ψ^3 are supplied by `data.mat`, where they are respectively saved as `tpsi1`, `tpsi2` and `tpsi3`.

The code of the function `triangle_quad` is as follows.

```
function ML = triangle_quad(Bl,s,psi1,psi2,psi3,areal,p_I)
ML = ( 8*areal*areal/((4-2*s)*(3-2*s)*(2-2*s)) ).*reshape(...
  psi1*( ( sum( (Bl*[p_I'; ones(1,length(p_I))]).^2 ).^(-1-s) )' ) +...
  psi2*( ( sum( (Bl*[ones(1,length(p_I)) ; p_I']).^2 ).^(-1-s) )' ) + ...
  psi3*( ( sum( (Bl*[p_I' ; p_I' - ones(1,length(p_I))]).^2 ).^(-1-s) )' ) ...
  , 3 , 3);
end
```

The matrix `Bl` plays the role of B_ℓ, `s` is s, `areal` is $|T_\ell|$, and `p_I` contains the values of the quadrature points in $[0,1]$. The latter are stored in `data.mat` under the same name, see Appendix C.1. The matrices Ψ^1, Ψ^2 and Ψ^3 are respectively saved as `psi1`, `psi2` and `psi3`.

The output `ML` of this function is a 3×3 matrix, such that: `ML` $\approx I_{\ell,\ell}$.

A.5. **Complement.** Recall that we are assuming that the domain Ω is contained in a ball $B = B(0, R)$. Here we are considering the interaction of two basis functions φ_i, φ_j such that $\mathrm{supp}(\varphi_i) \cap \mathrm{supp}(\varphi_j) = T_\ell$, over the region $T_\ell \times B^c$. Namely, we aim to compute

$$J_\ell = \int_{T_\ell} \int_{B^c} \frac{\varphi_i(x)\varphi_j(x)}{|x-y|^{2+2s}} \, dy dx = \int_{T_\ell} \varphi_i(x)\varphi_j(x)\psi(x) \, dx$$

$$= 2|T_\ell| \int_{\hat{T}} \hat{\varphi}_i(\hat{x})\hat{\varphi}_j(\hat{x})\psi(\chi_\ell(\hat{x})) \, d\hat{x},$$

where

$$\psi(x) = \int_{B^c} \frac{1}{|x-y|^{2+2s}} \, dy.$$

The integral above may be calculated by a Gauss quadrature rule in the reference element $\hat{T}$, provided that the values of ψ at the quadrature points are computed.

Observe that the function ψ is radial (see Figure 5) and therefore it suffices to estimate it on points of the form $x = (x_1, 0)$, where $x_1 > 0$. For a fixed point x and given $\theta \in [0, 2\pi]$, let $\rho_0(\theta)$ be the distance between x and the intersection of the ray starting from x with angle θ with respect to the horizontal axis. Then, it is simple to verify that

$$\rho_0(\theta, x) = -x_1 \cos\theta + \sqrt{R^2 - x_1^2 \sin^2\theta},$$

and therefore, integrating in polar coordinates,

$$\psi(x) = \frac{1}{2s} \int_0^{2\pi} \frac{1}{\rho_0(\theta, x)^{2s}} \, d\theta.$$
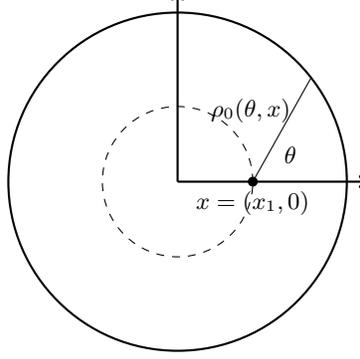
FIGURE 5. Computing $\psi(x)$ in a point of $B = B(0, R)$. Due to the symmetry, the value of ψ is the same along the dashed circle, hence we may assume that $x = (x_1, 0)$ and $0 \le x_1 < R$. For any $0 \le \theta \le \pi$, the function ρ_0 is given by $\rho_0(\theta, x) = -x_1 \cos\theta + \sqrt{R^2 - x_1^2 \sin^2\theta}$.

In order to compute J_ℓ we perform two nested quadrature rules: one over $\hat{T}$ and, for each quadrature point p_k in $\hat{T}$, another one to estimate $\psi(p_k)$ over $[0, 2\pi]$. We apply a 12 point quadrature formula over $\hat{T}$ and a 9 point one on $[0, 2\pi]$. Let $p_1, \ldots, p_{12} \in \hat{T}$, $\theta_1, \ldots, \theta_9 \in [0, 2\pi]$ be these quadrature nodes, and $w_1, \ldots, w_{12}$, $W_1, \ldots, W_9$ their respective weights. Applying the rules we obtain

$$J_\ell \approx \frac{|T_\ell|}{s} \sum_{k=1}^{12} w_k \hat{\varphi}_i(p_k) \hat{\varphi}_j(p_k) \sum_{q=1}^{9} \frac{W_q}{\rho_0(\theta_q, \chi_\ell(p_k))^{2s}}.$$

In the same fashion as for the other computations, we write the previous expression as the product of a pre-computed matrix (that only depends on the choice of the quadrature rules) times a vector that depends on the elements under consideration. Indeed, we define:

- A matrix $\Phi \in \mathbb{R}^{9 \times 12}$, such that

$$\Phi_{ij} = w_j \, \hat{\varphi}_{[i-1]_3+1}(p_j) \hat{\varphi}_{\lceil \frac{i}{3} \rceil}(p_j).$$

- A vector $\rho \in \mathbb{R}^{12}$, such that

$$\rho_k = \sum_q \frac{W_q}{\rho_0(\theta_q, \chi_\ell(p_k))^{2s}}.$$

Upon defining $\hat{J}_\ell := \Phi \cdot \rho$, we obtain

$$J_\ell^{[i-1]_3+1, \lceil \frac{i}{3} \rceil} \approx \frac{|T_\ell|}{s} \hat{J}_\ell^i, \ i \in \{1, ..., 9\}.$$

Using $MATLAB^{\circledR}$ notation, the above identity may be written as

$$J_\ell \approx \frac{|T_\ell|}{s} \texttt{reshape}(\hat{J}_\ell, \ 3 \ , \ 3).$$

The function `comp_quad` perform the previous computations.

```
function ML = comp_quad(Bl, x0, y0, s , phi , R, areal , p_I , w_I , p_T)
x = (Bl*p_T')' + [x0.*ones(length(p_T),1) , y0.*ones(length(p_T),1)];
aux = x(:,1)*cos(2*pi*p_I') + x(:,2)*sin(2*pi*p_I');
weight = ( ( -aux + sqrt( aux.^2 + R^2 - ( x(:,1).^2 +...
          x(:,2).^2 )*ones(1,length(p_I)) ) ).^(-2*s) )*w_I;
ML = (areal*2*pi/s).*reshape( phi*weight , 3 , 3);
end
```

Recall the parametrization $\chi_\ell(\hat{x}) = B_\ell\hat{x}+x_\ell^{(1)}$, so that $\mathtt{Bl}$, $\mathtt{x0}$ and $\mathtt{y0}$ satisfy $\mathtt{Bl} = B_\ell$ and $\begin{pmatrix} \mathtt{x0} \\ \mathtt{y0} \end{pmatrix} = x_\ell^{(1)}$. Moreover, $\mathtt{s}$ is s, $\mathtt{areal}$ is $|T_\ell|$, $\mathtt{p\_I}$ contains the quadrature points in the interval $[0,1]$, so that $2\pi\mathtt{p\_I}(q) = \theta_q$, $\mathtt{w\_I}(q) = W_q$, $\mathtt{p\_T}$ contains 12 quadrature points over $\hat{T}$, stored in $\mathtt{data.mat}$ as $\mathtt{p\_T\_12}$ (see Appendix C.1) and $\mathtt{phi}$ is the matrix Φ, that is pre-computed and stored in $\mathtt{data.mat}$ as $\mathtt{cphi}$ (see Appendix C.6).

The output $\mathtt{ML}$ satisfies $\mathtt{ML} \approx 2J_\ell$.

APPENDIX B. TWO AUXILIARY FUNCTIONS

The main code uses two functions that have not been outlined yet. Here we show them in detail.

The function $\mathtt{setdiff\_}$ takes as input two vectors $\mathtt{A}$ and $\mathtt{B}$, such that $\mathtt{A}$ contains consecutive positive integers, ordered low to high, $\mathtt{B}$ contains positive integers and is such that $\mathtt{length(B)} \leq \mathtt{length(A)}$ and $\mathtt{max(B)} \leq \mathtt{max(A)}$. The function computes the set difference $\mathtt{A} \setminus \mathtt{B}$, taking advantage of the pre-condition.

```
function e = setdiff_( A , B )
e = A;
b = B - A(1) + 1;
b( b<1 )=[];
e(b) = [];
end
```

On the other hand, the function $\mathtt{fquad}$ calculates the entries of the right hand side vector in (3.2). Taking as input $\mathtt{areal} := |T_\ell|$, the vectors $\mathtt{xl}$ and $\mathtt{yl}$, that contain the x and y coordinates of the vertices respectively, and a function f, $\mathtt{fquad}$ returns a vector in $\mathbb{R}^3$ array such that

$$\mathtt{fquad}_k \approx \int_{T_\ell} f\,\varphi_{i_k}.$$

Here, for $k \in \{1,2,3\}$, i_k denotes the index of the k-th vertex of T_ℓ and φ_{i_k} the basis function corresponding to it.

```
function VL = fquad( areal, xl , yl , f )
VL = zeros(3,1);
xmid = [(xl(2)+xl(3))/2, (xl(1)+xl(3))/2, (xl(1)+xl(2))/2];
ymid = [(yl(2)+yl(3))/2, (yl(1)+yl(3))/2, (yl(1)+yl(2))/2];
for i=1:3
    for j=1:3
        if j~=i
```

```
            VL(i) = VL(i) + areal/6 * f(xmid(j), ymid(j));
        end
    end
end
end
```

Appendix C. Auxiliary data

In order to perform the necessary calculations efficiently, along the execution the code makes use of pre-computed data, stored in `data.mat`. Here we describe the variables provided by this file. It is convenient to clarify that all the *MATLAB*® code showed in this section does not belong to the program itself. It is included with an illustrative purpose.

C.1. **Quadrature points and weights: p_cube, p_T, p_T_comp, p_I and w_I.** We list the quadrature points used in all the quadrature rules and their respective weights.

The matrix `p_cube` is used as input on functions `vertex_quad` and `edge_quad`, and contains 27 quadrature points over $[0, 1]^3$.

`p_cube =`

```
    0.1127    0.1127    0.1127
    0.1127    0.1127    0.5000
    0.1127    0.1127    0.8873
    0.1127    0.5000    0.1127
    0.1127    0.5000    0.5000
    0.1127    0.5000    0.8873
    0.1127    0.8873    0.1127
    0.1127    0.8873    0.5000
    0.1127    0.8873    0.8873
    0.5000    0.1127    0.1127
    0.5000    0.1127    0.5000
    0.5000    0.1127    0.8873
    0.5000    0.5000    0.1127
    0.5000    0.5000    0.5000
    0.5000    0.5000    0.8873
    0.5000    0.8873    0.1127
    0.5000    0.8873    0.5000
    0.5000    0.8873    0.8873
    0.8873    0.1127    0.1127
    0.8873    0.1127    0.5000
    0.8873    0.1127    0.8873
    0.8873    0.5000    0.1127
    0.8873    0.5000    0.5000
    0.8873    0.5000    0.8873
    0.8873    0.8873    0.1127
    0.8873    0.8873    0.5000
    0.8873    0.8873    0.8873
```

Over $\hat{T}$, we use two different quadrature rules, with 6 and 12 points. The set of nodes `p_T_6` is used to compute the non-touching element case and `p_T_12` as an input on `comp_quad`.

`p_T_6 =`

```
    0.5541     0.4459
    0.5541     0.1081
    0.8919     0.4459
    0.9084     0.0916
    0.9084     0.8168
    0.1832     0.0916
```

`p_T_12 =`

```
    0.7507     0.2493
    0.7507     0.5014
    0.4986     0.2493
    0.9369     0.0631
    0.9369     0.8738
    0.1262     0.0631
    0.6896     0.6365
    0.3635     0.0531
    0.9469     0.3104
    0.3635     0.3104
    0.6896     0.0531
    0.9469     0.6365
```

The 9×1 array `p_I` contains the quadrature points over $[0, 1]$, and `w_I` is a 9×1 array that contains their respective weights. These variables are used as input on `comp_quad`. The set of nodes `p_I` is also employed in `triangle_quad`.

`p_I =`   `w_I =`

```
    0.5000                          0.1651
    0.0820                          0.0903
    0.9180                          0.0903
    0.0159                          0.0406
    0.9841                          0.0406
    0.3379                          0.1562
    0.6621                          0.1562
    0.8067                          0.1303
    0.1933                          0.1303
```

C.2. **Auxiliary variables to compute non-touching elements case: `phiA`, `phiB` and `phiD`.** The variables `phiA`, `phiB` and `phiD` play the role of Φ^A, Φ^B and Φ^D (defined in Appendix A.1), respectively. We expose below the code used to set up these variables. We use the lists `p_T_6` and `w_T_6` of quadrature points and weights in $\hat{T}$ defined in Appendix C.1:

```
w_T_6 = zeros(6,1);
w_T_6(1) = 0.1117;
w_T_6(2) = w_T_6(1);
w_T_6(3) = w_T_6(1);
w_T_6(4) = 0.0550;
w_T_6(5) = w_T_6(4);
w_T_6(6) = w_T_6(4);

local = cell(1,6);
local{1} = @(x,y) 1-x;
local{2} = @(x,y) x-y;
local{3} = @(x,y) y;
local{4} = @(x,y) -(1-x);
local{5} = @(x,y) -(x-y);
local{6} = @(x,y) -y;

mat_loc = zeros(6);
for i = 1:6
    for j = 1:6
        mat_loc(i,j) = local{i}(p_T_6(j,1),p_T_6(j,2));
    end
end

W = w_T_6*(w_T_6');
M_aux = zeros(18);
N_aux = zeros(18);
L_aux = zeros(18);

phiB = zeros(9,36);
phiA = zeros(9,36);
phiD = zeros(9,36);

for i=1:3
    for j=1:3
        for k = 1:6
            for q=1:6
                M_aux( q + 6*(i-1) , k + 6*(j-1) ) =...
                W(q,k)*mat_loc(i,q)*mat_loc(j+3,k);
                N_aux( q + 6*(i-1) , k + 6*(j-1) ) =...
                W(q,k)*mat_loc(i,q)*mat_loc(j,q);
                L_aux( q + 6*(i-1) , k + 6*(j-1) ) =...
                W(q,k)*mat_loc(i+3,k)*mat_loc(j+3,k);
            end
        end
    end
end

for i=1:9
```

```
    [im jm] = ind2sub([3 3] , i);
    im = 6*(im - 1) + 1;
    jm = 6*(jm - 1) + 1;
    phiB(i,:) = reshape( M_aux( im:im+5 , jm:jm+5 ) , 1 , [] );
    phiA(i,:) = reshape( N_aux( im:im+5 , jm:jm+5 ) , 1 , [] );
    phiD(i,:) = reshape( L_aux( im:im+5 , jm:jm+5 ) , 1 , [] );
end
```

C.3. **Auxiliary variables to compute vertex-touching elements case:** vpsi1
and vpsi2. The variables vpsi1 and vpsi2 are used as arguments of the function
vertex_quad and play the role of the matrices Ψ^1 and Ψ^2 defined in Appendix A.2.
Below we show the code used to initialize these variables.

First we define a variable w_cube that lists the weights associated with each
quadrature point stored in p_cube:

```
w_cube =

    0.0214
    0.0343
    0.0214
    0.0343
    0.0549
    0.0343
    0.0214
    0.0343
    0.0214
    0.0343
    0.0549
    0.0343
    0.0549
    0.0878
    0.0549
    0.0343
    0.0549
    0.0343
    0.0214
    0.0343
    0.0214
    0.0343
    0.0549
    0.0343
    0.0214
    0.0343
    0.0214
```

The following lines generate vpsi1 and vpsi2:

```
psi_D1 = cell(5,1);
psi_D1{1} = @(x,y,z) y-1;
psi_D1{2} = @(x,y,z) 1-x;
```

```
psi_D1{3} = @(x,y,z)  x;
psi_D1{4} = @(x,y,z) -y.*(1-z);
psi_D1{5} = @(x,y,z) -y.*z;


psi_D2 = cell(5,1);
psi_D2{1} = @(x,y,z) -(y-1);
psi_D2{2} = @(x,y,z) y.*(1-z);
psi_D2{3} = @(x,y,z) y.*z;
psi_D2{4} = @(x,y,z) -(1-x);
psi_D2{5} = @(x,y,z) -x;


vpsi1 = zeros(25,27);
vpsi2 = zeros(25,27);


for i = 1:5
    for j = 1:5

        f1 = @(x,y,z) psi_D1{i}(x,y,z).*psi_D1{j}(x,y,z).*y;
        f2 = @(x,y,z) psi_D2{i}(x,y,z).*psi_D2{j}(x,y,z).*y;

        vpsi1( sub2ind([5 5], i , j) , : ) =...
        ( f1( p_cube(:,1) ,p_cube(:,2) , p_cube(:,3)) ).*w_cube;
        vpsi2( sub2ind([5 5], i , j) , : ) =...
        ( f2( p_cube(:,1) , p_cube(:,2) , p_cube(:,3)) ).*w_cube;

    end
end
```

C.4. **Auxiliary variables to compute edge-touching elements case: epsi1, ..., epsi5.** The variables epsi1, ..., epsi5 are used as input on the function edge_quad and play the role of Ψ^1, ..., Ψ^5 defined in Appendix A.3, respectively. The code employed to set up these variables is exhibited below. We used the variable w_cube defined in the previous sub-section (containing weights associated to quadrature points stored in p_cube):

```
psi_D1 = cell(3,1);
psi_D1{1} = @(x,y,z) -x.*y;
psi_D1{2} = @(x,y,z) x.*(1-z);
psi_D1{3} = @(x,y,z) x.*z;
psi_D1{4} = @(x,y,z) -x.*(1-y);


psi_D2 = cell(3,1);
psi_D2{1} = @(x,y,z) -x.*y.*z;
psi_D2{2} = @(x,y,z) -x.*(1-y);
psi_D2{3} = @(x,y,z) x;
psi_D2{4} = @(x,y,z) -x.*y.*(1-z);


psi_D3 = cell(3,1);
psi_D3{1} = @(x,y,z) x.*y;
```

```
psi_D3{2} = @(x,y,z) -x.*(1-y.*z);
psi_D3{3} = @(x,y,z) x.*(1-y);
psi_D3{4} = @(x,y,z) -x.*y.*z;


psi_D4 = cell(3,1);
psi_D4{1} = @(x,y,z) x.*y.*z;
psi_D4{2} = @(x,y,z) x.*(1-y);
psi_D4{3} = @(x,y,z) x.*y.*(1-z);
psi_D4{4} = @(x,y,z) -x;


psi_D5 = cell(3,1);
psi_D5{1} = @(x,y,z) x.*y.*z;
psi_D5{2} = @(x,y,z) -x.*(1-y);
psi_D5{3} = @(x,y,z) x.*(1-y.*z);
psi_D5{4} = @(x,y,z) -x.*y;


epsi1 = zeros(16,27);
epsi2 = zeros(16,27);
epsi3 = zeros(16,27);
epsi4 = zeros(16,27);
epsi5 = zeros(16,27);


for i = 1:4
    for j = 1:4

        f1 = @(x,y,z) psi_D1{i}(x,y,z).*psi_D1{j}(x,y,z) .*(x.^2);
        f2 = @(x,y,z) psi_D2{i}(x,y,z).*psi_D2{j}(x,y,z) .* (x.^2).*y;
        f3 = @(x,y,z) psi_D3{i}(x,y,z).*psi_D3{j}(x,y,z) .* (x.^2).*y;
        f4 = @(x,y,z) psi_D4{i}(x,y,z).*psi_D4{j}(x,y,z) .* (x.^2).*y;
        f5 = @(x,y,z) psi_D5{i}(x,y,z).*psi_D5{j}(x,y,z) .* (x.^2).*y;

        epsi1( sub2ind([4 4], i , j) , : ) =...
        ( f1( p_cube(:,1) , p_cube(:,2) , p_cube(:,3)) ).*w_cube;
        epsi2( sub2ind([4 4], i , j) , : ) =...
        ( f2( p_cube(:,1) , p_cube(:,2) , p_cube(:,3)) ).*w_cube;
        epsi3( sub2ind([4 4], i , j) , : ) =...
        ( f3( p_cube(:,1) , p_cube(:,2) , p_cube(:,3)) ).*w_cube;
        epsi4( sub2ind([4 4], i , j) , : ) =...
        ( f4( p_cube(:,1) , p_cube(:,2) , p_cube(:,3)) ).*w_cube;
        epsi5( sub2ind([4 4], i , j) , : ) =...
        ( f5( p_cube(:,1) , p_cube(:,2) , p_cube(:,3)) ).*w_cube;

    end
end
```

C.5. **Auxiliary variables to compute identical elements case:** `tpsi1`, `tpsi2`
and `tpsi3`**.** Here, the variables `tpsi1`, `tpsi2` and `tpsi3` are used as inputs on the
function `triangle_quad` and play the role of the matrices Ψ^1, Ψ^2 and Ψ^3, defined

in Appendix A.4, respectively. We describe the code used to set up these variables, where we use the quadrature data `p_I` and `w_I` introduced in Appendix C.1:

```
lambda_D1 = cell(3,1);
lambda_D1{1} = @(z) -z;
lambda_D1{2} = @(z) -(1-z);
lambda_D1{3} = @(z) 1;


lambda_D2 = cell(3,1);
lambda_D2{1} = @(z) -1;
lambda_D2{2} = @(z) (1-z);
lambda_D2{3} = @(z) z;


lambda_D3 = cell(3,1);
lambda_D3{1} = @(z) z;
lambda_D3{2} = @(z) -1;
lambda_D3{3} = @(z) 1-z;


tpsi1 = zeros(9,9);
tpsi2 = zeros(9,9);
tpsi3 = zeros(9,9);


for i = 1:3
    for j = 1:3

        f1 = @(z) lambda_D1{i}(z).*lambda_D1{j}(z);
        f2 = @(z) lambda_D2{i}(z).*lambda_D2{j}(z);
        f3 = @(z) lambda_D3{i}(z).*lambda_D3{j}(z);

        tpsi1( sub2ind([3 3], i , j) , : ) =  f1( p_I ).*w_I;
        tpsi2( sub2ind([3 3], i , j) , : ) =  f2( p_I ).*w_I;
        tpsi3( sub2ind([3 3], i , j) , : ) =  f3( p_I ).*w_I;

    end
end
```

C.6. **Auxiliary variable to compute quadrature over complement: `cphi`.**
The matrix Φ, defined in Appendix A.5, is stored as the variable `cphi` and used as input on the function `comp_quad`. Before explaining the code we employed to build it, we define the 12 by 1 array `w_T_12` as the set of weights associated to the quadrature points stored in `p_T_12`:

```
w_T_12 =

    0.1168
    0.1168
    0.1168
    0.0508
    0.0508
    0.0508
```

```
    0.0829
    0.0829
    0.0829
    0.0829
    0.0829
    0.0829
```

Then, the following lines generate `cphi`:

```
local = cell(1,3);
local{1} = @(x,y) 1-x;
local{2} = @(x,y) x-y;
local{3} = @(x,y) y;

cphi = zeros(9,12);

for i = 1:3
    for j = 1:3

        f1 = @(z,y) local{i}(z,y).*local{j}(z,y);
        cphi( sub2ind([3 3], i , j) , : ) =...
        f1( p_T_12(:,1) , p_T_12(:,2) ).*w_T_12;

    end
end
```

Appendix D. Main Code

For the sake of the reader's convenience, we include here the main code described in Sections 4 and 5.

```
1 clc
2 s = 0.5;
3 f = @(x,y) 1;
4 cns = s*2^(-1+2*s)*gamma(1+s)/(pi*gamma(1-s));
5 load('data.mat');
6 nn = size(p,2);
7 nt = size(t,1)
8 uh = zeros(nn,1);
9 K  = zeros(nn,nn);
10 b  = zeros(nn,1);
11 % Compute areas
12 area = zeros(nt,1);
13 for i=1:nt
14     aux = p( : , t(i,:) );
15     area(i) = 0.5.*abs( det(  [ aux(:,1) - aux(:,3)...
                                   aux(:,2) - aux(:,3)]  ) );
16 end
17 % Build patches data structure
18 deg = zeros(nn,1);
```

```
19 for i=1:nt
20     deg( t(i,:) ) = deg( t(i,:) ) + 1;
21 end
22 patches = cell(nn , 1);
23 for i=1:nn
24     patches{i} = zeros( 1 , deg(i) );
25 end
26 for i=1:nt
27     patches{ t(i,1) }(end - deg( t(i,1) ) + 1) = i;
28     patches{ t(i,2) }(end - deg( t(i,2) ) + 1) = i;
29     patches{ t(i,3) }(end - deg( t(i,3) ) + 1) = i;
30     deg( t(i,:) ) = deg( t(i,:) ) - 1;
31 end
32 % Preallocate auxiliary memory
33 vl = zeros(6,2);
34 vm = zeros(6*nt,2);
35 norms = zeros(36,nt);
36 ML = zeros(6,6,nt);
37 empty = zeros(nt,1);
38 aux_ind = reshape( repmat( 1:3:3*nt , 6 , 1 ) , [] , 1 );
39 empty_vtx = zeros(2,3*nt);
40 BBm = zeros(2,2*nt);
41 for l=1:nt-nt_aux % Main Loop
42     edge =  [ patches{t(l,1)} patches{t(l,2)} patches{t(l,3)} ];
43     [nonempty M N] = unique( edge , 'first' );
44     edge(M) = [];
45     vertex = setdiff(  nonempty , edge  );
46     ll = nt - l + 1 - sum( nonempty>=l );
47     edge( edge<=l ) = [];
48     vertex( vertex<=l ) = [];
49     empty( 1:ll ) = setdiff_( 1:nt , nonempty );
50     empty_vtx(: , 1:3*ll) = p( : , t( empty(1:ll) , : )' );
51     nodl = t(l,:);
52     xl = p(1 , nodl); yl = p(2 , nodl);
53     Bl = [xl(2)-xl(1) yl(2)-yl(1); xl(3)-xl(2) yl(3)-yl(2)]';
54     b(nodl) = b(nodl) + fquad(area(l),xl,yl,f);
55     K(nodl, nodl) = K(nodl, nodl)...
 + triangle_quad(Bl,s,tpsi1,tpsi2,tpsi3,area(l),p_I)...
 + comp_quad(Bl,xl(1),yl(1),s,cphi,R,area(l),p_I,w_I,p_T_12);
56     BBm(:,1:2*ll) = reshape( [ empty_vtx( : , 2:3:3*ll )...
 -  empty_vtx( : , 1:3:3*ll ) ,  empty_vtx( : , 3:3:3*ll )...
 - empty_vtx( : , 2:3:3*ll ) ] , [] , 2)' ;
57     vl = p_T_6*(Bl') + [ ones(6,1).*xl(1) ones(6,1).*yl(1) ];
58     vm(1:6*ll,:) = reshape(...
 permute(...
 reshape( p_T_6*BBm(:,1:2*ll) , [6 1 2 ll] ) , [1 4 3 2] ) , [ 6*ll 2 ] )...
 + empty_vtx(: , aux_ind(1:6*ll) )';
59     norms(:,1:ll) = reshape( pdist2(vl,vm(1:6*ll,:)), 36 , [] ).^(-2-2*s);
```

```
60     ML(1:3,1:3,1:ll) =  reshape( phiA*norms(:,1:ll) , 3 , 3 , [] );
61     ML(1:3,4:6,1:ll) =  reshape( phiB*norms(:,1:ll) , 3 , 3 , [] );
62     ML(4:6,4:6,1:ll) =  reshape( phiD*norms(:,1:ll) , 3 , 3 , [] );
63     ML(4:6,1:3,1:ll) =  permute( ML(1:3,4:6,1:ll) , [2 1 3] );
64     % Assembling stiffness matrix
65     for m=1:ll
66         order = [nodl t( empty(m) , : )];
67         K(order,order) = K(order,order)...
                + ( 8*area(empty(m))*area(l) ).*ML(1:6,1:6,m);
68     end
69     for m=vertex
70         nodm = t(m,:);
71         nod_com = intersect(nodl, nodm);
72         order = [nod_com nodl(nodl~=nod_com) nodm(nodm~=nod_com)];
73         K(order,order) = K(order,order)...
 + 2.*vertex_quad(nodl,nodm,nod_com,p,s,vpsi1,vpsi2,area(l),area(m),p_cube);
74     end
75     for m=edge
76         nodm = t(m,:);
77         nod_diff = [setdiff(nodl, nodm) setdiff(nodm, nodl)];
78         order = [ nodl( nodl~=nod_diff(1) ) nod_diff  ];
79         K(order,order) = K(order,order)...
 + 2.*edge_quad(...
nodl,nodm,nod_diff,p,s,epsi1,epsi2,epsi3,epsi4,epsi5,area(l),area(m),p_cube);
80     end
81 end
82 uh(nf) = ( K(nf,nf)\b(nf) )./cns;
83 trimesh(t(1:nt - nt_aux , :), p(1,:),p(2,:),uh);
```

References

[1] P. J. Acklam. *MATLAB array manipulation tips and tricks*. Notes, 2003.

[2] G. Acosta and J. P. Borthagaray. A fractional Laplace equation: Regularity of solutions and finite element approximations. *SIAM J. Numer. Anal.*, 55(2):472–495, 2017.

[3] G. Acosta, J. P. Borthagaray, O. Bruno, and M. Maas. Regularity theory and high order numerical methods for the (1d)-Fractional Laplacian. To appear in Math. Comp., 2017.

[4] J. Alberty, C. Carstensen, and S. A. Funken. Remarks around 50 lines of Matlab: short finite element implementation. *Numer. Algorithms*, 20(2-3):117–137, 1999.

[5] J. Bertoin. *Lévy processes*, volume 121 of *Cambridge Tracts in Math.* Cambridge University Press, Cambridge, 1996.

[6] J. P. Borthagaray, L. M. Del Pezzo, and S. Martínez. Finite element approximation for the fractional eigenvalue problem. Preprint, arXiv, 2016.

[7] S. Chaturapruek, J. Breslau, D. Yazdi, T. Kolokolnikov, and S. G. McCalla. Crime modeling with Lévy flights. *SIAM J. Appl. Math.*, 73(4):1703–1720, 2013.

[8] M. D'Elia and M. Gunzburger. The fractional Laplacian operator on bounded domains as a special case of the nonlocal diffusion operator. *Comp. Math. Appl.*, 66(7):1245 – 1260, 2013.

[9] B. Dyda, A. Kuznetsov, and M. Kwaśnicki. Fractional Laplace operator and Meijer G-function. *Constr. Approx.*, 45(3):427–448, 2017.

[10] G. Grubb. Fractional Laplacians on domains, a development of Hörmander's theory of μ-transmission pseudodifferential operators. *Adv. Math.*, 268:478 – 528, 2015.

[11] Y. Huang and A. M. Oberman. Numerical methods for the fractional Laplacian: A finite difference-quadrature approach. *SIAM J. Numer. Anal.*, 52(6):3056–3084, 2014.

[12] T. A. M. Langlands, B. I. Henry, and S. L. Wearne. Fractional cable equation models for anomalous electrodiffusion in nerve cells: finite domain solutions. *SIAM J. Appl. Math.*, 71(4):1168–1203, 2011.

[13] X. Ros-Oton and J. Serra. The Dirichlet problem for the fractional Laplacian: Regularity up to the boundary. *J. Math. Pures Appl. (9)*, 101(3):275 – 302, 2014.

[14] L. Rosasco, M. Belkin, and E. De Vito. On learning with integral operators. *J. Mach. Learn. Res.*, 11:905–934, 2010.

[15] S. A. Sauter and C. Schwab. *Boundary element methods*, volume 39 of *Springer Ser. Comput. Math.* Springer-Verlag, Berlin, 2011. Translated and expanded from the 2004 German original.

[16] M. I. Višik and G. I. Èskin. Convolution equations in a bounded region. *Uspekhi Mat. Nauk*, 20(3 (123)):89–152, 1965. English translation in *Russian Math. Surveys*, 20:86-151, 1965.

(G. Acosta, F. M. Bersetche and J. P. Borthagaray) IMAS - CONICET AND DEPARTAMENTO DE MATEMÁTICA, FCEyN - UNIVERSIDAD DE BUENOS AIRES, CIUDAD UNIVERSITARIA, PABELLÓN I (1428) BUENOS AIRES, ARGENTINA.

E-mail address, G. Acosta: `gacosta@dm.uba.ar`

URL, G. Acosta: `http://mate.dm.uba.ar/~gacosta/`

E-mail address, F. M. Bersetche: `fbersetche@dm.uba.ar`

E-mail address, J.P. Borthagaray: `jpbortha@dm.uba.ar`